

Synthesis and Characterization of High Affinity Fluorogenic α -Synuclein Probes

Zsolia Lengyel-Zhand^{1†}, John J Ferrie^{2†}, Bieneke Janssen¹, Chia-Ju Hsieh¹, Thomas Graham¹, Kuiying Xu¹, Conor M. Haney², Virginia M.-Y. Lee³, John Q. Trojanowski³, E. James Petersson^{2*} and Robert H. Mach^{1*}

¹Department of Radiology, Perelman School of Medicine, University of Pennsylvania, Philadelphia, PA 19104, United States

²Department of Chemistry, University of Pennsylvania, Philadelphia, Pennsylvania 19104, United States

³Department of Pathology and Laboratory Medicine, Perelman School of Medicine, University of Pennsylvania, Philadelphia, PA 19104, United States

Electronic Supplementary Information

Table of Contents

I.	Experimental Section.....	S2-8
II.	LCMS Chromatogram and ¹ H and ¹³ C Spectrum of Tg-47	S9-10
III.	LCMS Chromatogram and ¹ H and ¹³ C Spectrum of Tg-49	S11-12
IV.	LCMS Chromatogram and ¹ H and ¹³ C Spectrum of Tg-51	S13-14
V.	LCMS Chromatogram, and ¹ H and ¹³ C Spectrum of Tg-52	S14-15
VI.	LCMS Chromatogram, and ¹ H and ¹³ C Spectrum of Tg-53	S16-17
VII.	LCMS Chromatogram, and ¹ H and ¹³ C Spectrum of Tg-54	S17-18
VIII.	Figures S1-2.....	S19
IX.	Table S1 and Figure S3	S20
X.	Figure S4-7 and Table S2-3.....	S21-25
XI.	Table S4 and Figures S8-9	S26-27
XII.	Figures S10-S12	S28-30
XIII.	References	S31

General chemistry. Chemicals were obtained from commercial sources and used without further purification. Solvents were purchased from commercial sources and used as received unless stated otherwise. Reactions were performed at room temperature unless stated otherwise. Reactions were monitored by thin layer chromatography (TLC) on pre-coated silica 60 F254 aluminum plates (MilliporeSigma, Burlington, MA, USA), spots were visualized by UV light. Evaporation of solvents was performed under reduced pressure at 40 °C using a rotary evaporator. Flash column chromatography was performed on a Biotage® (Charlotte, NC, USA) Isolera One system equipped with Biotage® SNAP KP-Sil cartridges. Nuclear magnetic resonance (NMR) spectroscopy was performed on a Bruker (Billerica, MA, USA) Avance Neo 400 (400.17 MHz for ¹H and 100.63 MHz for ¹³C) or a Bruker Avance Neo 600 (600.13 MHz for ¹H and 150.90 MHz for ¹³C) with chemical shifts (δ) reported in parts per million (ppm) relative to the solvent ((CD₃)₂SO, ¹H 2.50 ppm, ¹³C 39.52 ppm) or tetramethylsilane (TMS, ¹H and ¹³C 0.00 ppm). Purity of the compounds was determined by high performance liquid chromatography (HPLC) using a Waters (Milford, MA, USA) e2695 instrument equipped with an Agilent (Santa Clara, CA, USA) Eclipse XDB-C18 (5 μ m, 100 x 4.6 mm) column. HPLC mobile phase was 0.1M ammonium formate buffer (pH 4.5)/acetonitrile (50:50 for **Tg-47** and **Tg-54**; 40:60 for **Tg-49** and **Tg-51-53**), run at a flow rate of 1.5 mL/min. Detection wavelength was 254 nm. Low resolution (LR) Liquid Chromatography Mass Spectrometry (LCMS) was carried out using a Waters SQD equipped with an Acquity UPLC instrument in positive ion mode. High resolution LCMS (HRMS) for accurate mass measurement was carried out using a Waters LCT Premier XE instrument in positive ion mode. Abbreviation: 'Tg' is the initials of the chemist (Thomas Graham) who originally made these compounds.

(Z)-5-Hydroxy-2-((E)-3-(4-methoxyphenyl)allylidene)benzofuran-3(2H)-one (Tg-47)

A slurry of 5-hydroxybenzofuran-3-one (465 mg, 3.10 mmol) and 4-methoxycinnamaldehyde (502 mg, 3.10 mmol) in 95% EtOH (20 mL) was treated with 3 mL of conc. HCl (~13 M) and heated to 70 °C. The solids rapidly dissolve and over the course of the reaction (3h) a thick orange precipitate was formed. The mixture was allowed to cool to room temperature and filtered. The collected solids were rinsed with MeOH (2-3 mL) and dried under vacuum to afford the desired product as a bright orange solid (475 mg, 52% yield).

¹H NMR (400 MHz, (CD₃)₂SO) δ 9.73 (s, 1H), 7.62 (d, *J* = 8.6 Hz, 2H), 7.32 (d, *J* = 8.8 Hz, 1H), 7.11-7.27 (m, 3H), 6.97-6.99 (m, 3H), 6.80 (d, *J* = 11.1 Hz, 1H), 3.80 (s, 3H); ¹³C NMR (100 MHz, (CD₃)₂SO) δ 182.64, 160.44, 158.46, 153.61, 146.89, 141.82, 129.21, 128.81, 125.39, 122.24, 118.06, 114.51, 114.30, 113.62, 107.46, 55.31; LRMS (ESI) *m/z* calcd. for C₁₈H₁₄O₄, 294.0892; found, 295.4 [M+H]⁺; HRMS (ESI) *m/z* calcd. for C₁₈H₁₄O₄, 294.0892; found, 295.0989 [M+H]⁺.

(Z)-2-((E)-3-(4-Methoxyphenyl)allylidene)-3-oxo-2,3-dihydrobenzofuran-5-yl trifluoromethanesulfonate (Tg-49). A slurry of **Tg-47** (294 mg, 1.0 mmol) in CH₂Cl₂ (10 mL) was treated with pyridine (500 μ L, 4.0 mmol) and cooled to 0 °C in an ice bath. A solution of Tf₂O (1 mL, 1M in CH₂Cl₂) was added dropwise over the course of 5 min. The ice bath was removed, and the reaction was stirred at room temperature for 30 min. The reaction mixture was quenched with 1 N HCl (10 mL) and diluted with CH₂Cl₂ (20 mL). The layers were separated, and the organics dried (Na₂SO₄) and concentrated to give the desired product as an orange solid (400 mg, 94% yield). The material was used without further purification.

¹H NMR (400 MHz, (CD₃)₂SO) δ 7.96 (d, *J* = 2.4 Hz, 1H), 7.92 (dd, *J* = 9.0, 2.5 Hz, 1H), 7.69 (d, *J* = 8.9 Hz, 1H), 7.65 (d, *J* = 8.5 Hz, 1H), 7.37 (d, *J* = 15.4 Hz, 1H), 7.16-7.23 (m, 1H), 6.96-

7.00 (m, 3H), 3.81 (s, 3H); ¹³C NMR (100 MHz, (CD₃)₂SO) δ 181.02, 163.07, 160.78, 146.50, 144.79, 143.64, 129.96, 129.54, 128.62, 123.05, 117.78, 117.24, 116.75, 115.20, 114.59, 55.35; LRMS (ESI) *m/z* calcd. for C₁₉H₁₃F₃O₆S, 426.0385; found, 427.4 [M+H]⁺; HRMS (ESI) *m/z* calcd. for C₁₉H₁₃F₃O₆S, 426.0385; found, 427.0485 [M+H]⁺.

General Procedure for Suzuki Cross coupling with Aryl triflates. A vial was sequentially charged with **Tg-49** (1 eq.), Pd G2 XPhos (5 mol%), K₃PO₄ (2 eq.) and (hetero)aryl boronic acid (2 eq.). The vial was briefly purged with N₂ and sealed with a septum-lined screw-cap. Degassed 1,4-dioxane/H₂O (4:1; 8 mL/mmol) was added *via* syringe and the reaction heated to 50 °C for 20 mins. The reaction mixture was then diluted with CH₂Cl₂ (100 mL) and H₂O (15 mL). The layers were separated, and the aqueous phase extracted with CH₂Cl₂ (2 x 50 mL). The pooled organics were dried (Na₂SO₄) and concentrated under reduced pressure to give the crude product that was further purified *via* flash column chromatography.

(Z)-2-((E)-3-(4-methoxyphenyl)allylidene)-5-(2-methoxypyrimidin-5-yl)benzofuran-3(2H)-one (Tg-51). The title compound was obtained with (2-methoxypyrimidin-5-yl)boronic acid via the general procedure. Flash column chromatography (gradient of 12-100% EtOAc in hexanes) yielded **Tg-51** as a slightly orange solid (68 mg, 76% yield).

¹H NMR (400 MHz, (CD₃)₂SO) δ 9.00 (s, 2H), 8.12-8.14 (m, 2H), 7.61-7.65 (m, 3H), 7.18-7.34 (m, 2H), 7.01 (d, *J* = 8.5 Hz, 2H), 6.94 (d, *J* = 11.1 Hz, 1H), 3.97 (s, 3H), 3.81 (s, 3H); ¹³C NMR (150 MHz, (CD₃)₂SO) δ 182.53, 165.04, 164.74, 161.09, 157.96, 146.85, 143.19, 135.93, 131.93, 129.86, 129.21, 126.80, 123.17, 122.23, 118.40, 115.92, 115.04, 114.23, 55.82, 55.24; HPLC purity: 73%; LRMS (ESI) *m/z* calcd. for C₂₃H₁₈N₂O₄, 386.1267; found, 387.5 [M+H]⁺; HRMS (ESI) *m/z* calcd. for C₂₃H₁₈N₂O₄, 386.1267; found, 387.1349 [M+H]⁺.

(Z)-2-((E)-3-(4-Methoxyphenyl)allylidene)-3-oxo-2,3-dihydrobenzofuran-5-yl trifluoromethanesulfonate (Tg-52). The title compound was obtained with (6-methoxypyridin-3-yl)boronic acid via the general procedure. Flash column chromatography (gradient of 6-50% EtOAc in hexanes) yielded **Tg-52** as a slightly orange solid (73 mg, 80% yield). ¹H NMR (400 MHz, (CD₃)₂SO) δ 8.53 (d, *J* = 2.0 Hz, 1H), 8.10 (td, *J* = 8.7, 2.2 Hz, 2H), 8.00 (s, 1H), 7.65 (d, *J* = 8.5 Hz, 2H), 7.59 (d, *J* = 8.6 Hz, 1H), 7.18-7.33 (m, 2H), 7.00 (d, *J* = 8.5 Hz, 2H), 6.89-6.93 (m, 2H), 3.81 (s, 3H), 3.90 (s, 3H); ¹³C NMR (150 MHz, (CD₃)₂SO) δ 182.23, 164.00, 163.17, 160.62, 146.48, 144.86, 142.61, 137.77, 135.55, 132.83, 129.83, 128.78, 128.11, 122.61, 121.36, 117.99, 115.29, 114.59, 113.62, 110.67, 55.37, 53.36; HPLC purity: 93%; LRMS (ESI) *m/z* calcd. for C₂₄H₁₉NO₄, 385.1314; found, 386.5 [M+H]⁺; HRMS (ESI) *m/z* calcd. for C₂₄H₁₉NO₄, 385.1314; found, 386.1399 [M+H]⁺.

(Z)-2-((E)-3-(4-methoxyphenyl)allylidene)-5-(pyridin-3-yl)benzofuran-3(2H)-one (Tg-53)

The title compound was obtained with pyridin-3-ylboronic acid via the general procedure. Flash column chromatography (gradient of 30-100% EtOAc in hexanes) yielded **Tg-53** as a slightly orange solid (21 mg, 49% yield). ¹H NMR (400 MHz, (CD₃)₂CO) δ 8.94 (d, *J* = 2.0 Hz, 1H), 8.61 (dd, *J* = 1.5, 4.8 Hz, 1H), 8.10-8.13 (m, 2H), 8.03 (d, *J* = 2.0 Hz, 1H), 7.67 (td, *J* = 2.0, 8.8 Hz, 2H), 7.57 (d, *J* = 8.6 Hz, 1H), 7.47-7.51 (m, 1H), 7.27-7.28 (m, 2H), 7.02 (td, *J* = 2.0, 8.8 Hz, 2H), 6.83-6.85 (m, 1H), 3.86 (s, 3H); ¹³C NMR (100 MHz, (CD₃)₂CO) δ 183.12, 165.87, 162.03, 149.66, 148.90, 147.93, 142.99, 136.62, 135.93, 135.01, 134.41, 130.11, 130.09, 124.61, 124.10, 123.04, 118.94, 115.58, 115.35, 114.44, 55.79; HPLC purity: 95%; LRMS (ESI) *m/z* calcd. for

C₂₃H₁₇NO₃, 355.1208; found, 356.5 [M+H]⁺; HRMS (ESI) *m/z* calcd. for C₂₃H₁₇NO₃, 355.1208; found, 356.1298 [M+H]⁺.

(Z)-2-((E)-3-(4-methoxyphenyl)allylidene)-3-oxo-2,3-dihydrobenzofuran-5-yl

methylcarbamate (Tg-54). A slurry of Tg-47 (294 mg, 1.0 mmol) in CH₂Cl₂ (10 mL) was treated with TEA (420 μL, 3 mmol) and DMAP (~5 mg, cat.). N-methylcarbamoyl chloride (140 mg, 1.5 mmol) was added in one portion and the reaction allowed to stir for 2 h. The reaction mixture was directly purified by flash column chromatography (gradient of 21-44% EtOAc in hexanes) to afford the desired product as a yellow solid (172 mg, 49% yield). ¹H NMR (400 MHz, (CD₃)₂CO) δ 7.65 (td, *J* = 8.8, 1.9 Hz, 2H), 7.44-7.49 (m, 2H), 7.40 (d, *J* = 8.8 Hz, 1H), 7.23-7.25 (m, 2H), 7.01 (td, *J* = 8.8, 1.9 Hz, 2H), 6.77-6.80 (m, 2H), 3.86 (s, 3H), 3.81 (s, 3H); ¹³C NMR (150 MHz, (CD₃)₂CO) δ 183.02, 162.98, 161.99, 155.78, 148.23, 142.83, 139.97, 131.91, 131.55, 130.06, 123.51, 118.96, 117.10, 115.45, 115.33, 114.06, 55.77, 27.75; HPLC purity: 95%; LRMS (ESI) *m/z* calcd. for C₂₀H₁₇NO₅, 351.1107; found, 352.5 [M+H]⁺; HRMS (ESI) *m/z* calcd. for C₂₀H₁₇NO₅, 351.1107; found, 352.1191 [M+H]⁺.

α-Syn protein expression and purification. The plasmid encoding the human α-Syn sequence¹ with a C-terminal intein fusion was transformed into *Escherichia coli* BL21(DE3) and the cells were grown on agar/LB plates with ampicillin (100 μg/mL) overnight at 37 °C. The next day a single colony was inoculated into 100 mL Luria-Bertani (LB) containing ampicillin (100 μg/mL). The culture was incubated at 37 °C overnight with shaking at ~200 rpm. The following day, 10 mL of the overnight culture was diluted with 1 L of LB media supplemented with ampicillin and this culture was incubated at 37°C until OD₆₀₀ reached 0.6 – 0.7. Protein expression was induced by addition of isopropyl-β-D-thiogalactoside (IPTG) to a final concentration of 1 mM and continued to grow at 18 °C overnight. After induction, cells were harvested by centrifugation at 4 °C (20 min, 4,000g). The typical yield of wet-cell paste was 2 g/L.

Cells were suspended in a lysis buffer (5 mL for 1 g of cell paste) containing 25 mM Tris, 20 mM imidazole, 50 mM NaCl (pH 8) with a protease inhibitor (phenylmethylsulfonyl fluoride, 0.5 mM final concentration and protease inhibitor cocktail from Cell Signaling Technology). Cells were lysed by sonication on ice for 10 min (20 s on, 20 s off). The crude cell lysate was then centrifuged at 20,000g for 30 min, and the supernatant was mixed with Ni-NTA resin (Clontech, 3 mL) and kept on a rocker at room temperature for 30 min. The resin was then washed with 100 mL wash buffer (25 mM Tris, 20 mM imidazole, 50 mM NaCl, pH 8). The protein was eluted with a buffer containing 25 mM Tris, 300 mM imidazole, 50 mM NaCl (pH 8). Fractions containing the protein were identified by UV-Vis spectroscopy, combined and was treated with β-mercaptoethanol (200 mM final concentration) overnight at room temperature to cleave the C-terminal intein. The next day, the protein was concentrated to 3 mL and dialyzed against buffer containing 25 mM Tris, 50 mM NaCl, pH 8. After dialysis, the protein mixture was loaded onto Ni-NTA column and the pure α-Syn protein was collected in the flow through fractions. The combined protein fractions were concentrated and dialyzed against buffer containing 50 mM Tris, 150 mM NaCl, pH 7.5. The purity of the protein was confirmed by SDS-PAGE. Protein concentration was determined by measuring the absorbance at 280 nm and using the calculated (ExpASy) extinction coefficient of 5960 M⁻¹cm⁻¹.

Preparation of α -Syn fibrils. Purified α -Syn monomer (100 μ M) was incubated in buffer containing 50 mM Tris (pH 7.5), 150 mM NaCl and 0.05% NaN₃ for 72 hours at 37 °C with shaking at 1000 rpm in a Fisher Scientific Mixer.

Determination of Tg-Compound Absorbance and Emission Spectra. All absorbance spectra were collected on a Thermo Scientific Genesys 150 UV-Visible Light Spectrophotometer (Waltham, MA, USA), while fluorescence spectra were collected either on a Photon Technologies International (PTI) QuantaMaster40 fluorometer (currently Horiba Scientific, Edison, NJ, USA) or Tecan Infinite M1000 PRO plate reader (San Jose, CA, USA). Lifetimes were collected on the PTI QuantaMaster40 with a 483 nm LED light source. Plate reader measurements were performed in Greiner black, clear bottom, half-area, 96-well plates. Stocks of **Tg-51-54** compounds were prepared in DMSO and used for all experiments described below.

Determination of the Effect of Solvent Polarity on Tg-Compound Absorbance and Fluorescence Spectra. The absorbance spectra of Tg-51-54 were acquired in solvents with varying polarities. Measurements were taken at 20 μ M concentrations of each compound in the 50:50 buffer/DMSO using 20 mM Tris, 100 mM NaCl, pH 7.4 as the buffer, 100 % DMSO, 95 % water and 95 % ethanol, with DMSO making up the remaining 5 % in the latter solvent conditions. Following the collection of absorbance spectra using the Thermo Scientific Genesys, fluorescence spectra were acquired using the same set of solvent conditions at 5 μ M concentrations of the compounds. All fluorescence spectra were acquired on the M1000 plate reader via top-reads at a 2 nm step size, 20 μ s integration time, 50 flashes per measurement, with 5 nm slit widths with a 438 nm excitation, monitoring the emission from 450 – 700 nm.

Determination of Tg-Compound Extinction Coefficient. The extinction coefficient for each compound was determined via eight-point serial dilution of each compound into 50:50 buffer/DMSO using 20 mM Tris, 100 mM NaCl, pH 7.4 as the buffer. All spectra were acquired on the Thermo Scientific Genesys at a 2 nm step size using the “medium” scan rate, measuring from 250 – 650 nm. The extinction coefficient for each compound was computed from the compound specific maximum absorbance between 325 – 500 nm. All compounds fit well to a line; however, the **Tg-53** compound may be subject to aggregation as the zero-point concentration for the linear fit does not track through a zero-absorbance value. As a result, the computed y-intercept for the **Tg-53** fit is provided in addition to the slope of the linear range.

Determination of Tg-Compound Fluorescence Binding and Turn-On. Binding affinities and fluorescence turn-on of each compound were assessed by measuring the emission of 1 μ M of each compound in the presence of varying concentrations of α -Syn fibrils. All measurements were taken in 20 mM Tris, 100 mM NaCl, pH 7.4 with 2% DMSO. Excitation and emission spectra of each compound in the presence and absence of fibrils were collected at each compound’s excitation (for emission spectra) and emission (for excitation spectra) maxima. All spectra were acquired on the M1000 plate reader via top-reads at a 2 nm step size, 20 μ s integration time, 50 flashes per measurement, with 5 nm slit widths. Binding curves plotting the total intensity from either excitation or emission spectra, determined by computing the area under each curve, as a function of α -Syn fibril concentration were fit to the one site – specific binding – saturation model in GraphPad Prism 7.04 (San Diego, CA, USA) detailed below (Equation 1.):

$$(1) \text{ Total Intensity} = B_{max} \frac{X}{X + K_d}$$

In the above equation B_{max} is the maximum emission of the compound when fully bound, K_d is the dissociation constant and X is the concentration of fibrillized α -Syn. Although this does not directly report on the dissociation constant of the compound for fibrils, the assay demonstrates that the compound's fluorescence turn-on is dependent on fibril binding and serves as a comparative metric of the relative binding affinities of each compound for α -Syn fibrils.

Determination of Tg-Compound Quantum Yield. Quantum yields for each compound bound to fibrils were determined via comparison to thioflavin T (ThT). Each compound was incubated at 1 μ M with 98 μ M α -Syn fibrils in 20 mM Tris, 100 mM NaCl, pH 7.4 with 2% DMSO. Absorbance spectra of each compound bound to fibrils were collected using 98 μ M fibrillized α -Syn in buffer as the subtracted background. The relative absorbance of each compound compared to the absorbance of ThT was employed alongside the published extinction coefficient of ThT bound to α -Syn fibrils to compute approximate fibril-bound extinction coefficients for each compound.² Emission spectra were acquired for each sample via excitation at 440 nm, measuring the emission from 460 – 650 nm using 5 nm excitation and emission slit widths and a 0.25 second integration time. Relative total intensities were computed by integrating the emission intensity over all wavelengths and ratiometrically correcting for the absorbance of each compound at 440 nm, determined separately. Following correction, the quantum yield (ϕ_{Tg}) was computed by multiplying the quantum yield of ThT by the ratio of the emission intensities for the compound and ThT, $\phi_{Tg} = \phi_{ThT} * (I_{Tg}/I_{ThT})$. The published quantum yield of ThT bound to α -Syn fibrils is 0.13.²

Determination of Tg-Compound Lifetime. Fluorescence lifetimes were acquired using a pulsed LED with a 483 nm emission maximum passed through a 500 nm cutoff short pass filter on the PTI QuantaMaster40. All data were collected at an emission wavelength of 525 nm with 25 nm slit widths, a 199 ns collection time parsed into 4096 bins and a maximum single bin count number of 10,000. Following acquisition, all lifetimes were fit to a single exponential decay using a sample containing only α -Syn fibrils to collect the instrument response function. Lifetimes were collected on samples containing compounds and α -Syn fibrils prepared identically to those detailed above for determining the quantum yield.

Competition binding assay. α -Syn fibrils (200 nM for site 2 and 50 nM for site 9) were mixed with [³H]-**Tg-190b** (11 nM) or [³H]-**BF2846** (4 nM) and varying concentrations of cold compounds. The K_d of [³H]-**BF2846** for α -Syn fibrils is 2.0 nM. Competitors were diluted in 50 mM Tris-HCl buffer (pH 7.4). Nonspecific binding was determined in reactions containing cold **Tg-190b** (2 μ M) or **BF2846** (0.5 μ M). Reactions were incubated at 37 °C for 1 hour before quantifying bound radioligand. Bound and free radioligand were separated by vacuum filtration through Whatman GF/C filters (Brandel) in a 24-sample harvester system (Brandel), followed by washing with buffer containing 50 mM Tris-HCl (pH 7.4) and 150 mM NaCl. Filters containing the bound ligand were mixed with 3 mL of scintillation cocktail (MicroScint-20, PerkinElmer Informatics, Inc.) and counted after 12 hours of incubation on a MicroBeta System (PerkinElmer Informatics, Inc.). All data points were measured in triplicates. IC_{50} and K_i values were calculated by fitting the data to Equations 2 and 3 below using GraphPad Prism software:

$$(2) \log EC_{50} = \log(10^{\log K_i} * (1 + [radioligand]/K_d))$$

$$(3) Y = \text{Bottom} + (\text{Top}-\text{Bottom}) / (1 + 10^{(X-\log EC_{50})})$$

Where $\log EC_{50}$ is the log of the concentration of competitor that results in binding half-way between Bottom and Top; $\log K_i$ is the log of the molar equilibrium dissociation constant of unlabeled ligand; [radioligand] is the concentration of radiolabeled ligand in nM; K_d is the equilibrium dissociation constant of the radioligand in nM; Top and Bottom are plateaus in the units of Y axis.

Postmortem human brain tissue collection. Donor brains subjects following neuropathological evaluation were selected from the brain bank at the Center for Neurodegenerative Disease Research at the University of Pennsylvania based on previously published criteria.³ The protocols for brain harvesting, selection of areas to obtain tissue blocks and staining and diagnostic procedures followed have been previously reported in detail.

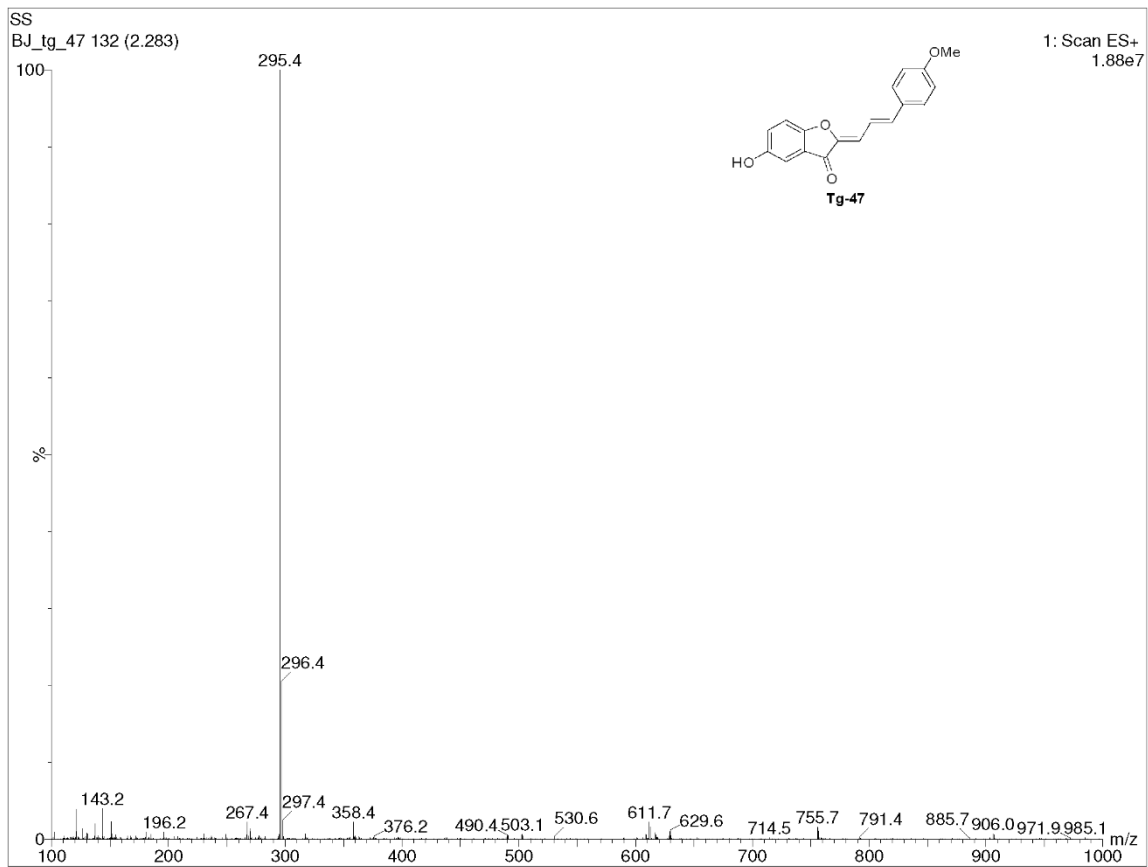
Pathology report for patients:

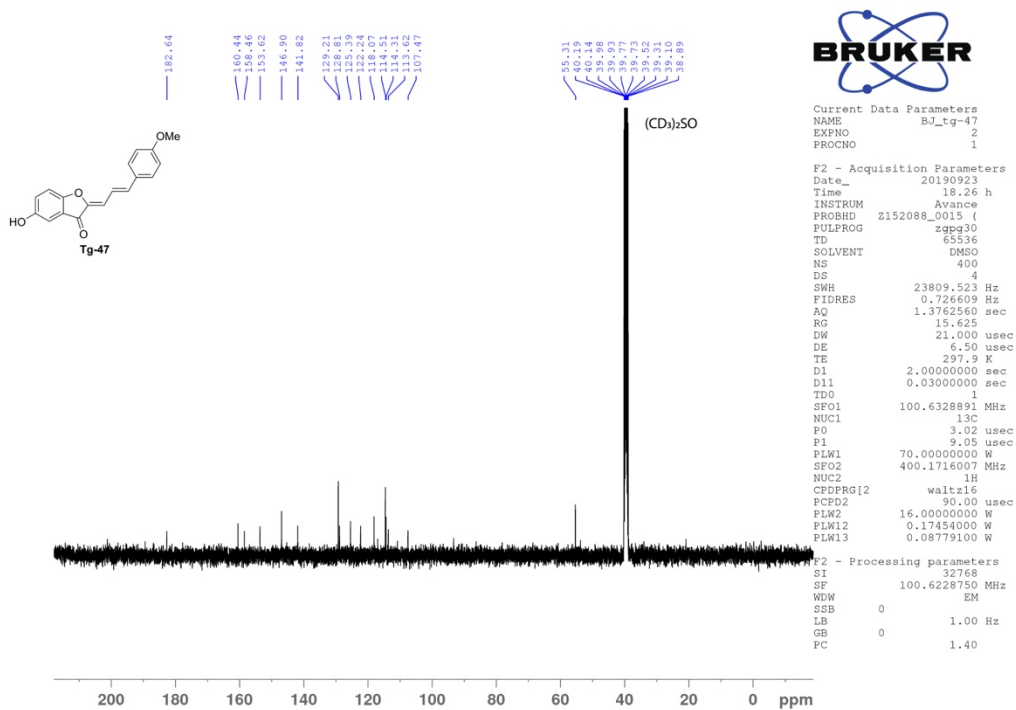
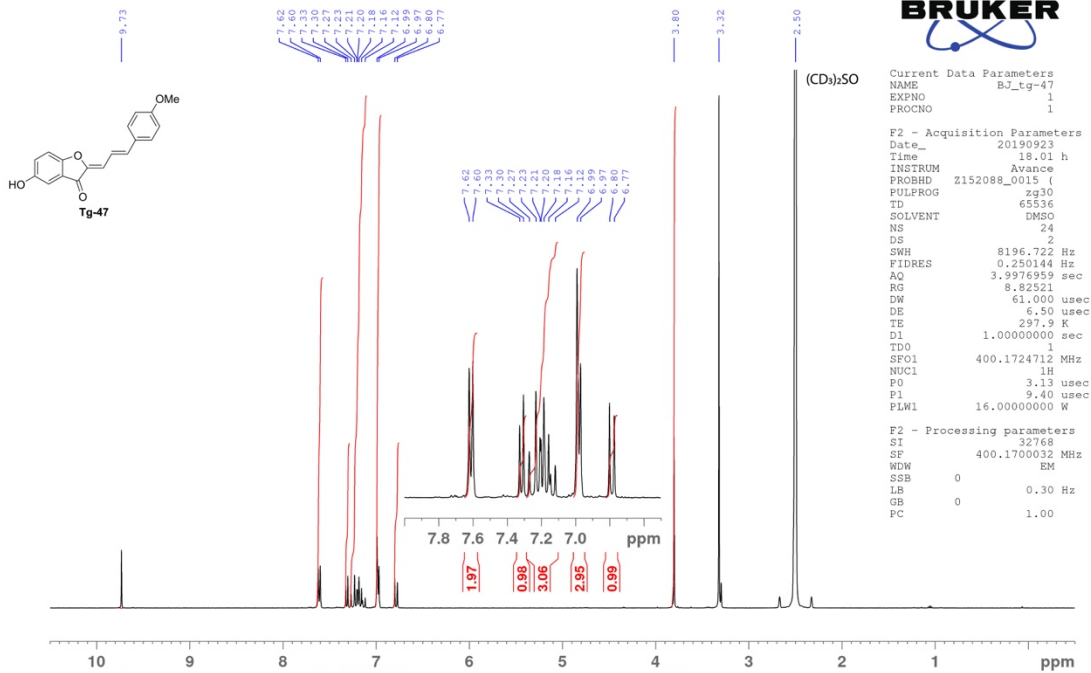
- PD patient: The major findings include Lewy body pathology in the substantia nigra, midbrain and dorsal medulla. Lewy bodies and Lewy neurites were also seen in the amygdala, hippocampus, frontal cortex, angular gyrus, cingulate cortex, thalamus and basal ganglia. Low density alpha-synuclein positive inclusions were also noted in the white matter. The postmortem finding of Lewy body pathology together with the clinical history, establish a diagnosis of Parkinson's disease. The absence of classical glial cytoplasmic inclusions along with the paucity of white matter inclusions do not support a definitive diagnosis of multiple system atrophy. The paucity of neurofibrillary tangles and the absence of senile plaques do not support the concurrent diagnosis of AD.
- MSA patient: The major finding is widespread alpha-synuclein positive glial cytoplasmic inclusions involving white matter, and to lesser extent in grey matter. The glial cytoplasmic inclusions are most abundant in the brainstem and cerebellum but could be found throughout the whole brain. Tau pathology, beta-amyloid plaques and TDP-43 inclusions are not seen. The neuropathologic findings are diagnostic of MSA.
- AD patient: The major findings included numerous beta-amyloid plaques, particularly in neocortical and limbic regions but also present in the brainstem and cerebellum. Amyloid angiopathy is present. No Lewy bodies, Lewy neurites or TDP-43 inclusions are seen. The Tau pathology and the beta-amyloid plaques present in the brain indicate a high level of Alzheimer's disease and correlate with the clinical history.

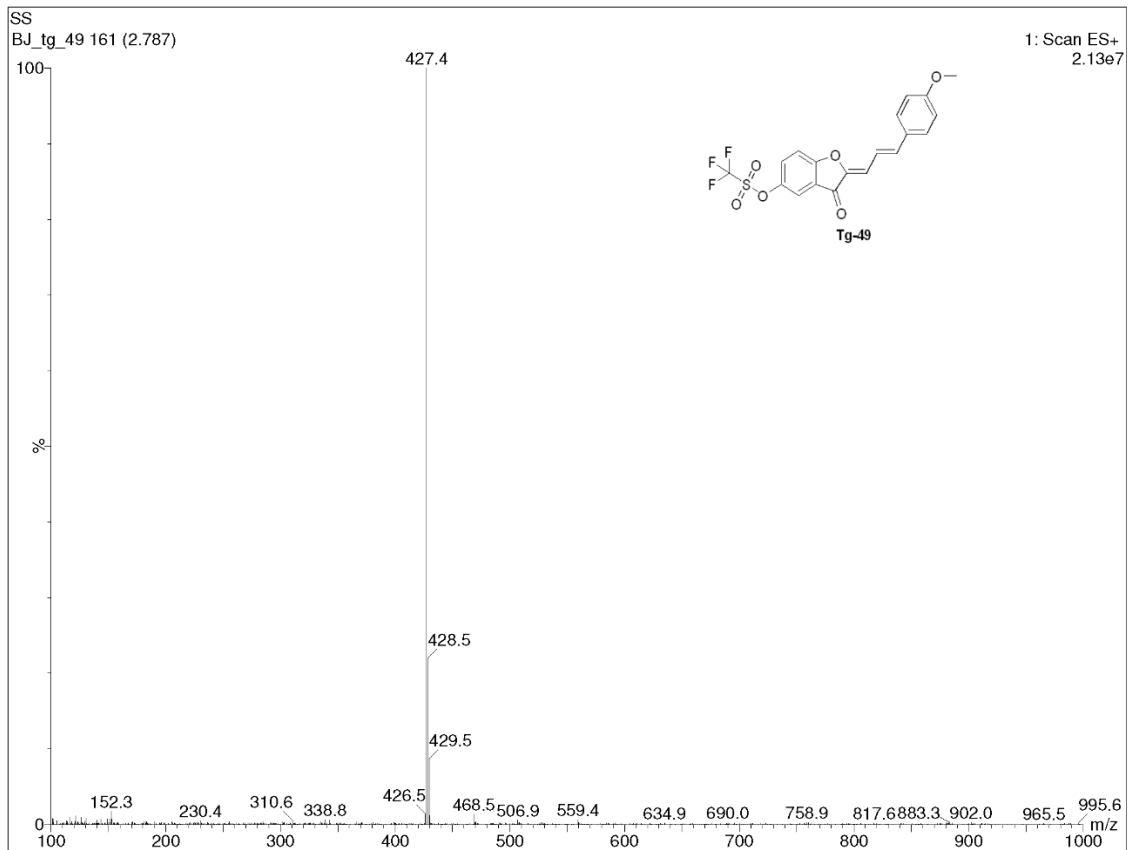
Immunofluorescence. Blocks of brain tissue from human PD, MSA and AD cases were frozen in optimal cutting temperature compound (OCT, Tissue-Tek, Sakura Finetek, USA). The frozen tissue was sliced into 10 μM thick sections in a Leica CM1950 cryostat and mounted onto Apex Superior Adhesive slides (Leica). Sections were fixed with 4% paraformaldehyde in PBS, washed with PBS three-times, then permeabilized with 0.1% Triton X-100 in PBS. After washing with PBS, tissue was stained with TrueBlack Lipofuscin Autofluorescence Quencher (Biotium), following manufacturer's instructions. Sections were blocked with 10% normal goat serum (Fisher Scientific) at room temperature for 1 hour, then incubated with primary $\alpha\text{-Syn}$ antibody (for PD and MSA tissues, Syn303 from BioLegend, 1:200 in 1% BSA in PBS) or $\text{a}\beta$ antibody (for AD tissue, 6A10 from BioLegend 1:200 in 1% BSA in PBS) overnight at 4 °C. After three washes

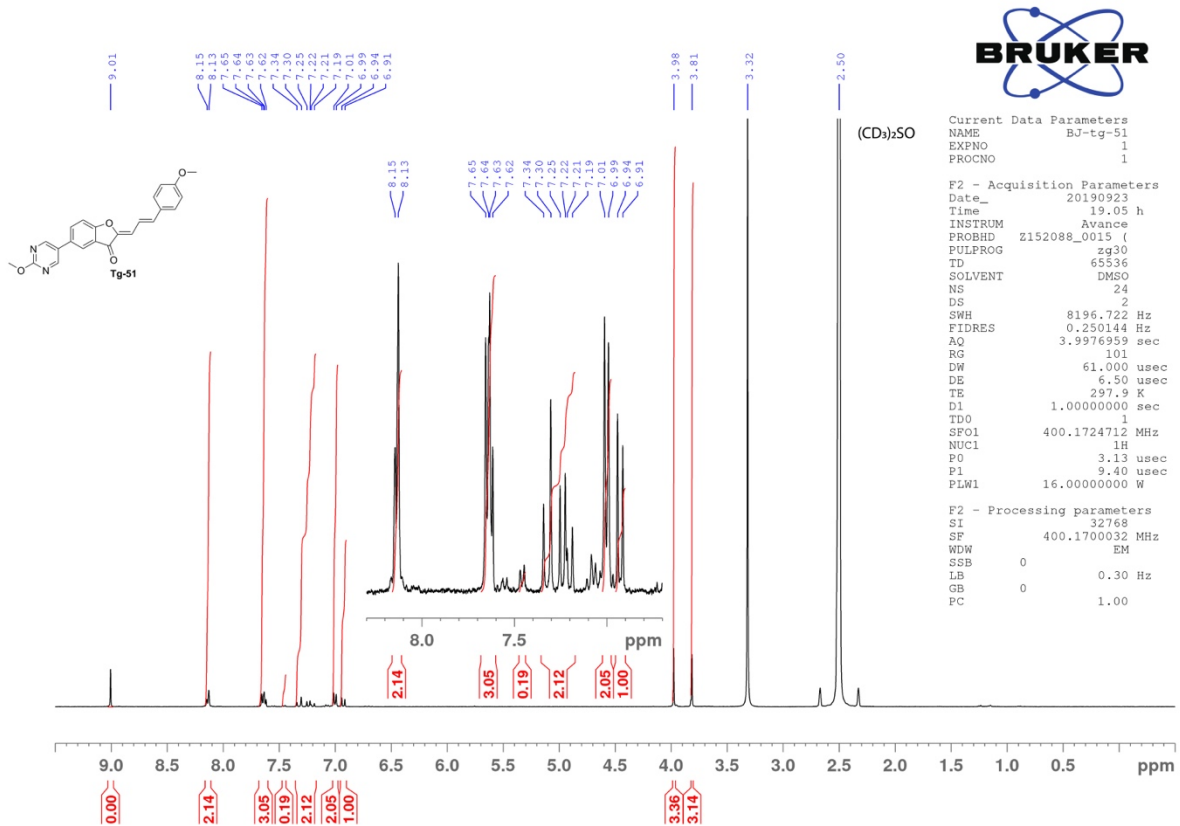
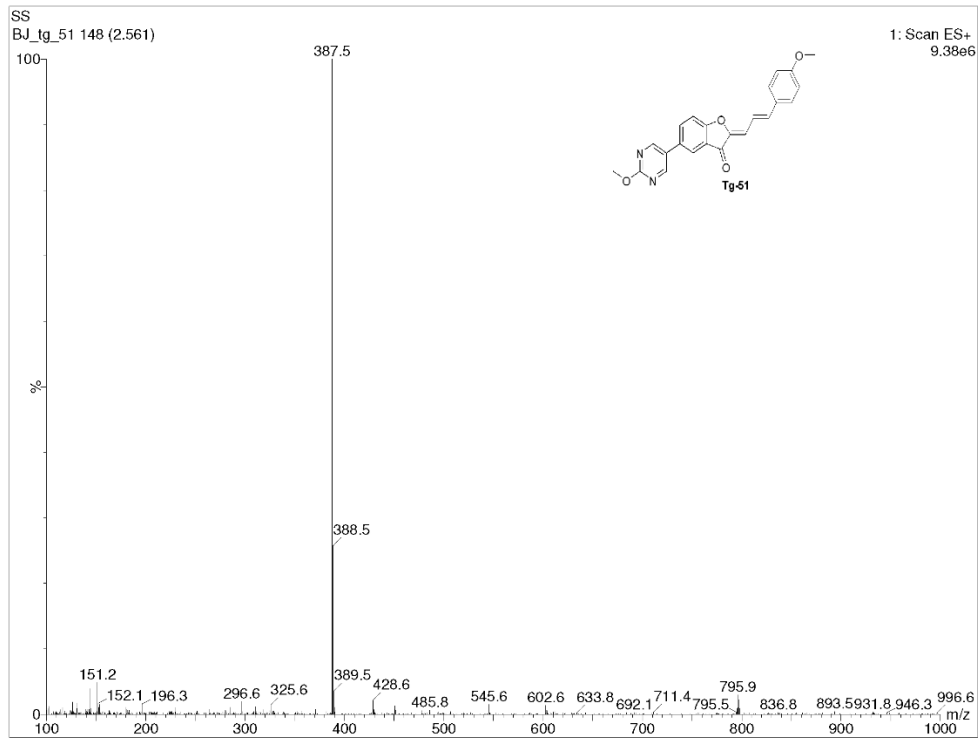
with PBS, the tissue was incubated with a secondary antibody labeled with Alexa Fluor 647 (1:200 in 1% BSA in PBS) for 1 hour at room temperature. Tissue was then treated with **Tg-52**. Each section was incubated at room temperature for 2 hours with 10 μM of compound in PBS (with 3% DMSO), washed with PBS three times and mounted on a coverslip. The fluorescent images were acquired by a Zeiss Axio Imager M2 microscope.

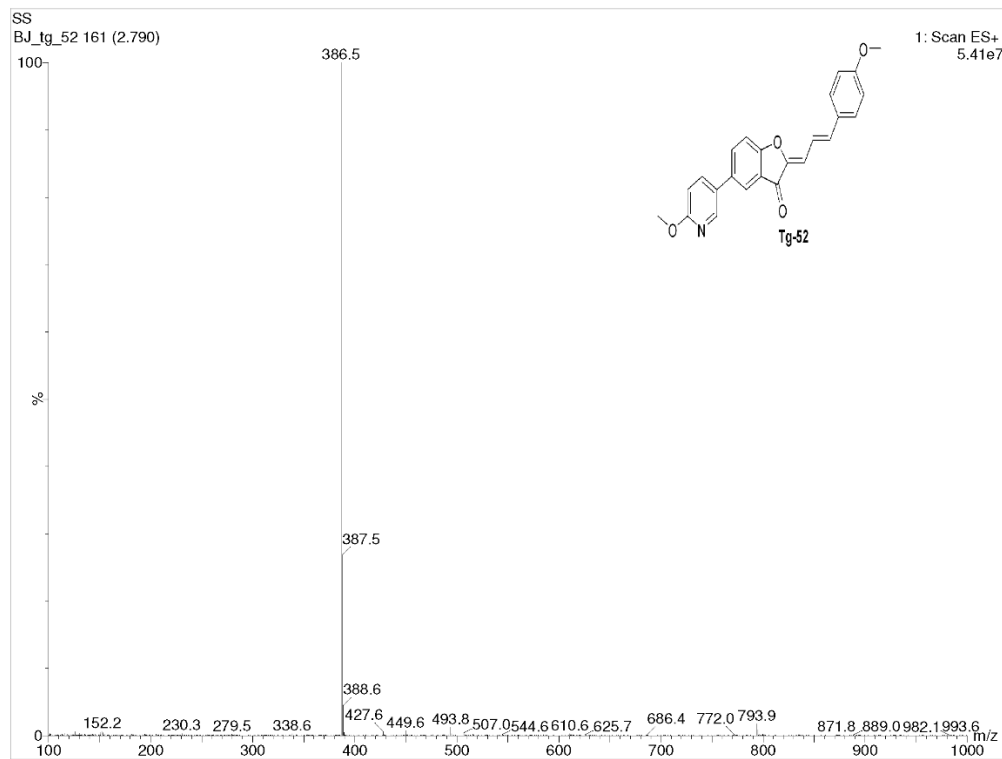
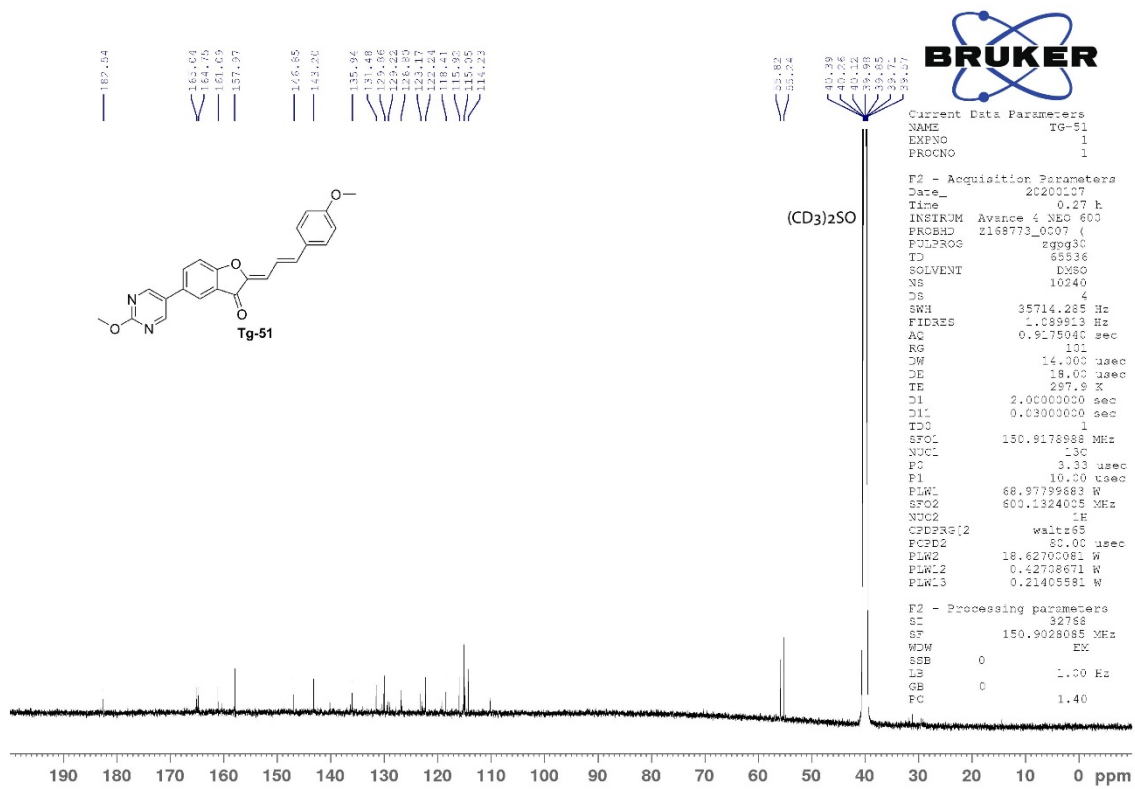
Molecular Docking, *In silico* molecular docking study was performed following the previously published protocol.⁴ The structures of **Tg-51-54** were drawn in ChemDraw Professional 15.1 (PerkinElmer Informatics, Inc.), then imported to Chem3D Ultra 15.1 (PerkinElmer Informatics, Inc.) to obtain the MMFF94 minimized **Tg-51-54** structures prepared for molecular docking. Molecular blind docking was performed via the AutoDock 4.2 plugin for PyMOL (pymol.org).⁵ The solid-state NMR structure of full-length α -Syn fibril (PDB ID: 2N0A) was obtained from the RCSB protein data bank (<https://www.rcsb.org/>) as a target protein for blind docking. Non-polar hydrogens were removed from both compounds and protein structures. A grid box with a dimension of $95 \times 50 \times 95 \text{ \AA}^3$ was applied to the α -Syn fibril structure. The Lamarckian Genetic Algorithm with a maximum of 2,500,000 energy evaluations was used to calculate 1,000 protein-ligand binding poses for each compound. The % probability, predicted best binding energy, and average binding energy of each binding site that determined from blind docking were reported.



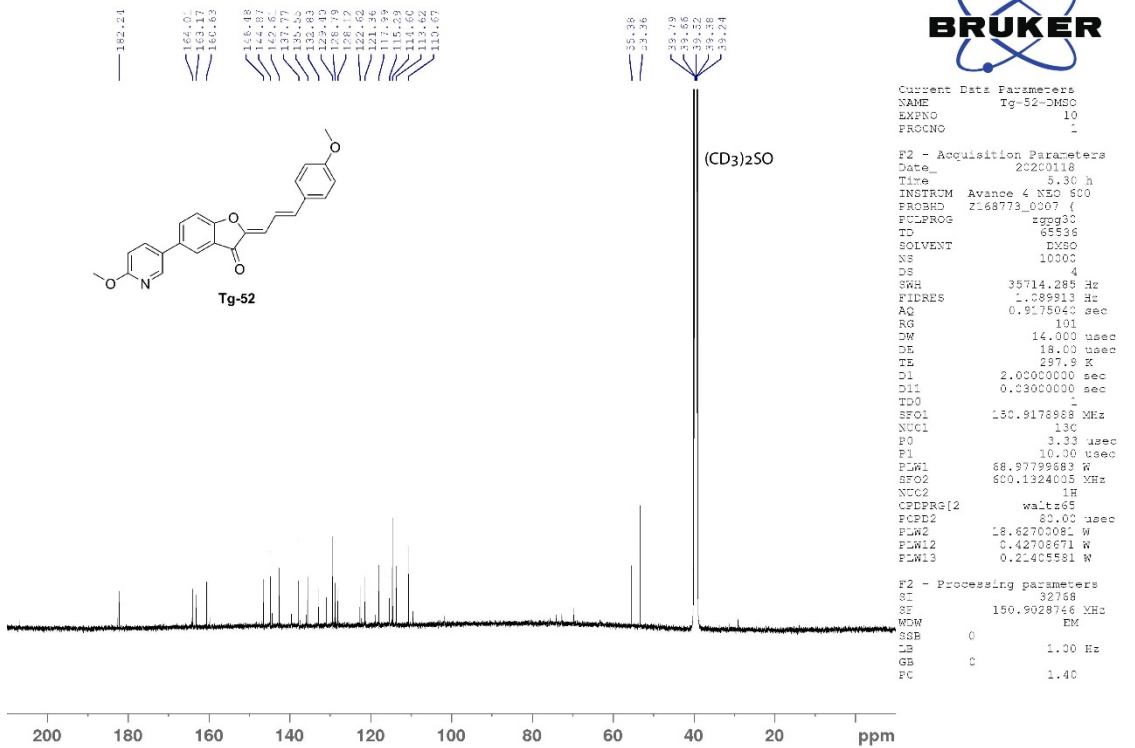
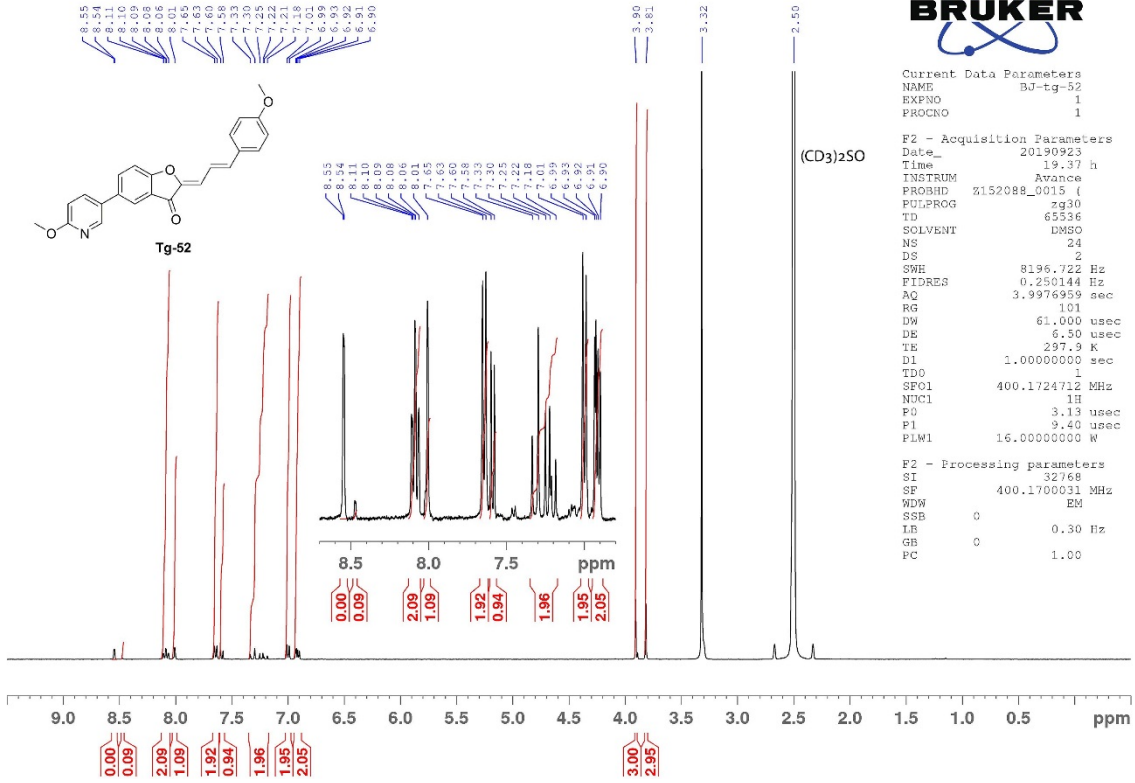


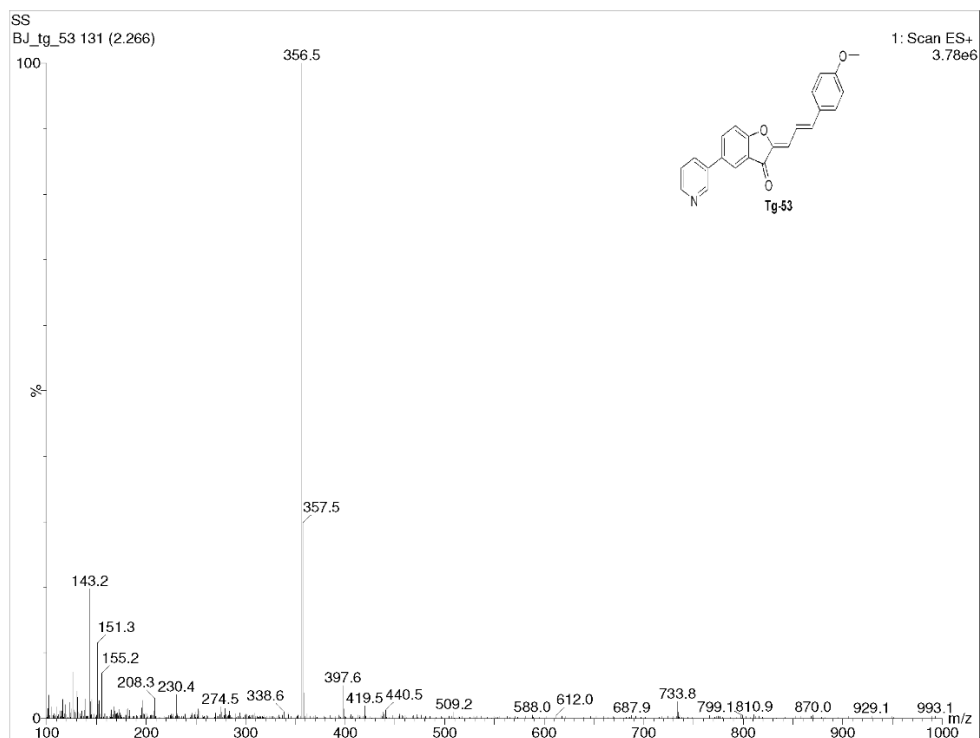




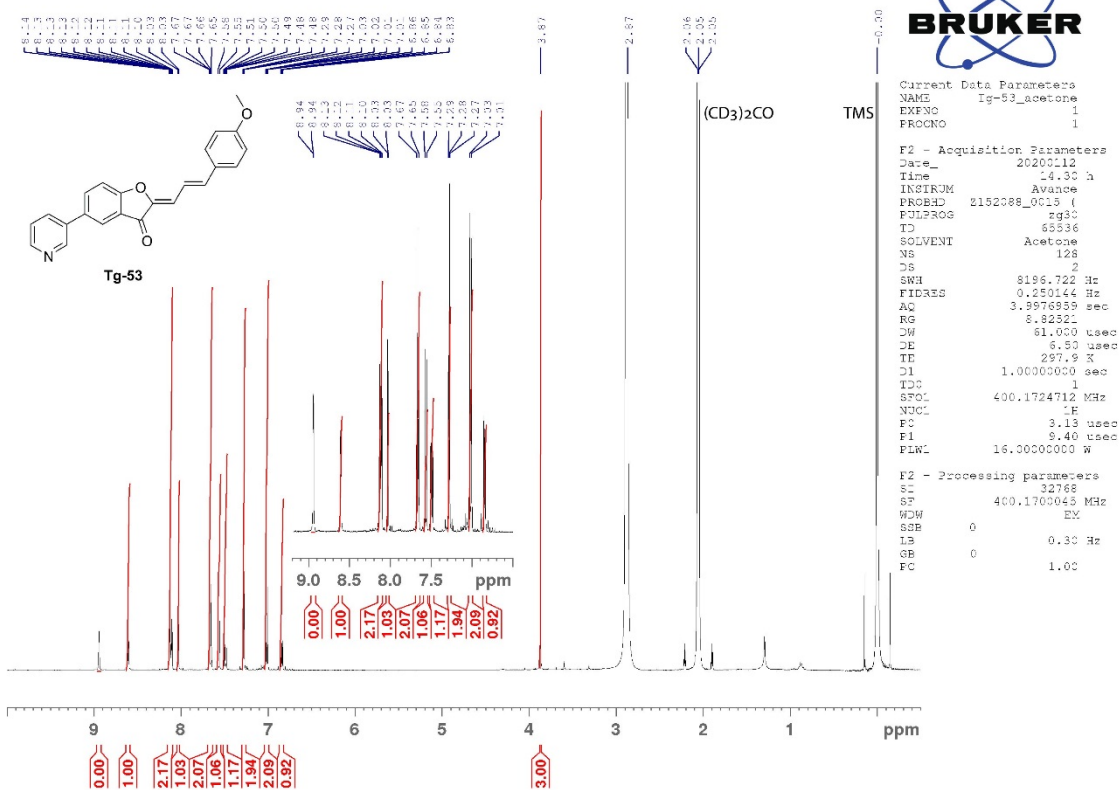


S

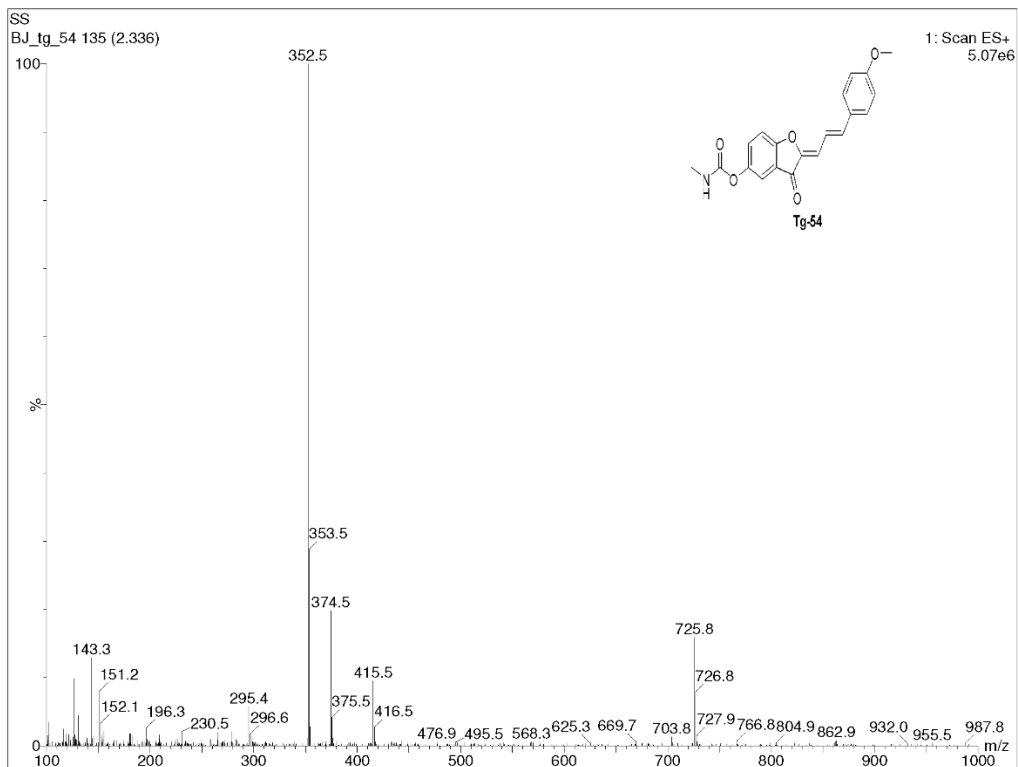
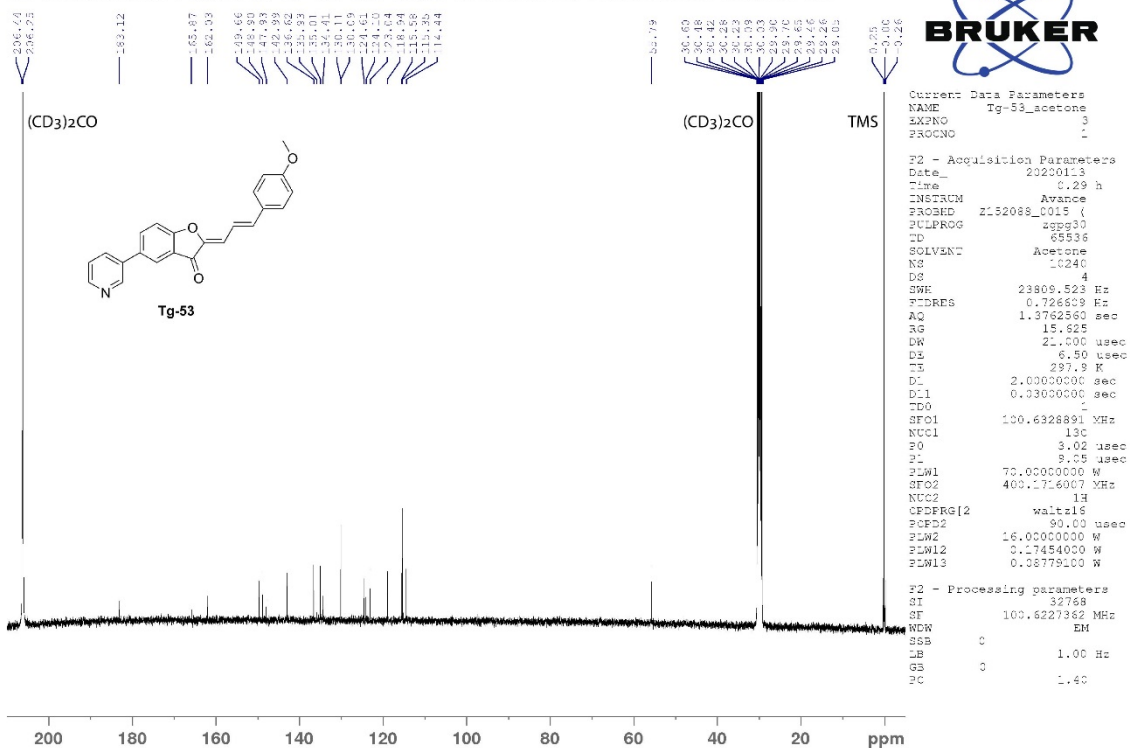


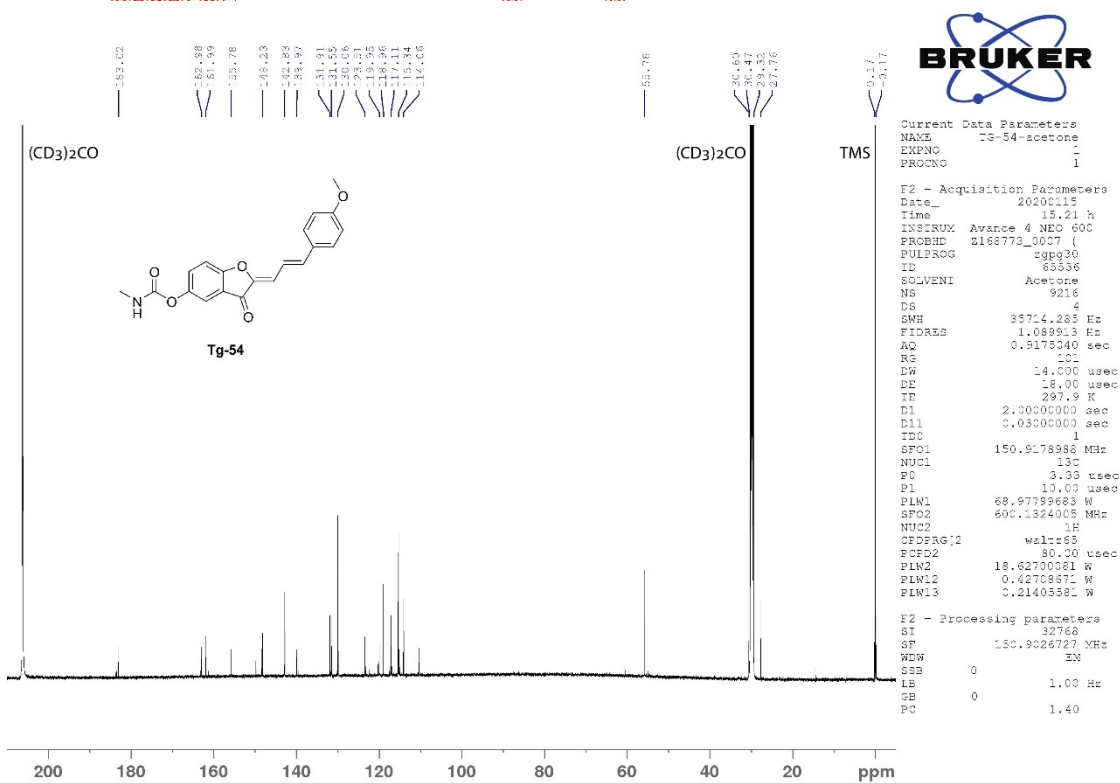
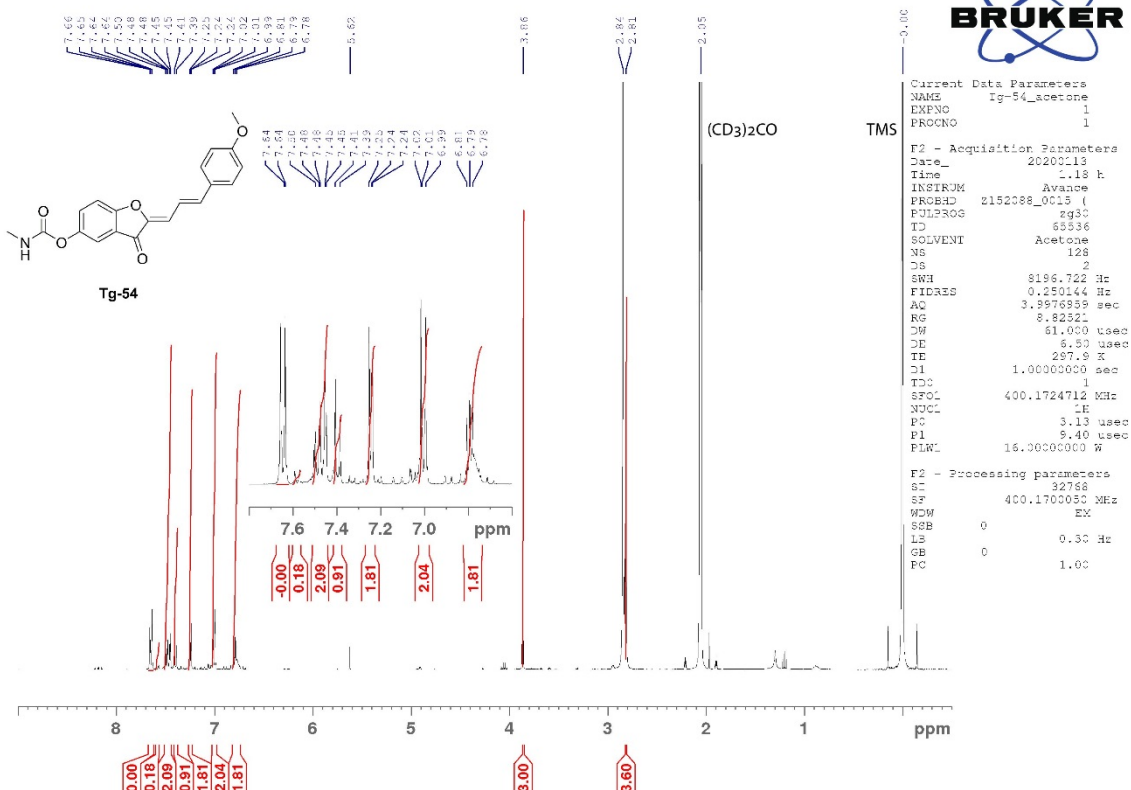


Instrumentation supported by the NSF Major Research Instrumentation Program (aw.



Instrumentation supported by the NSF Major Research Instrumentation Program (aw.





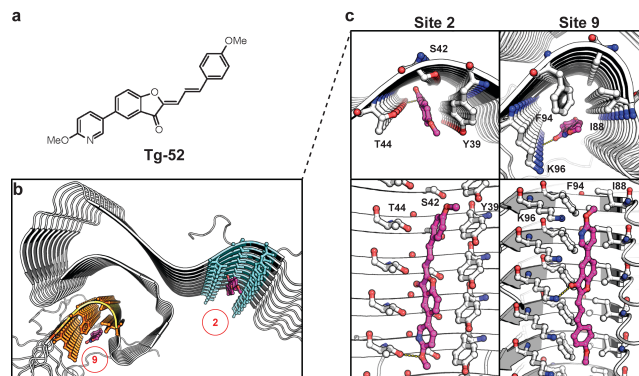


Figure S1. (a) Molecular structure of **Tg-52**. (b) Solid-state NMR structure of α -Syn showing two binding sites for small molecules (cyan: site 2, orange: site 9). (c) Docking of **Tg-52** to site 2 (left) and site 9 (right) in α -Syn fibrils.

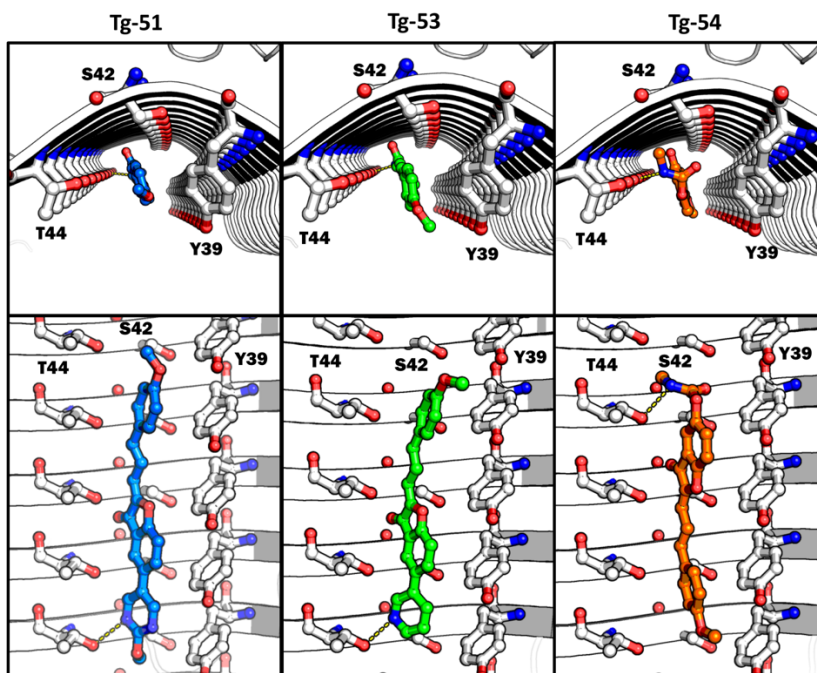


Figure S2. Docking of **Tg-51**, **Tg-53** and **Tg-54** binding to site 2 in α -Syn, viewed from the fibril axis (top) and from the side (bottom).

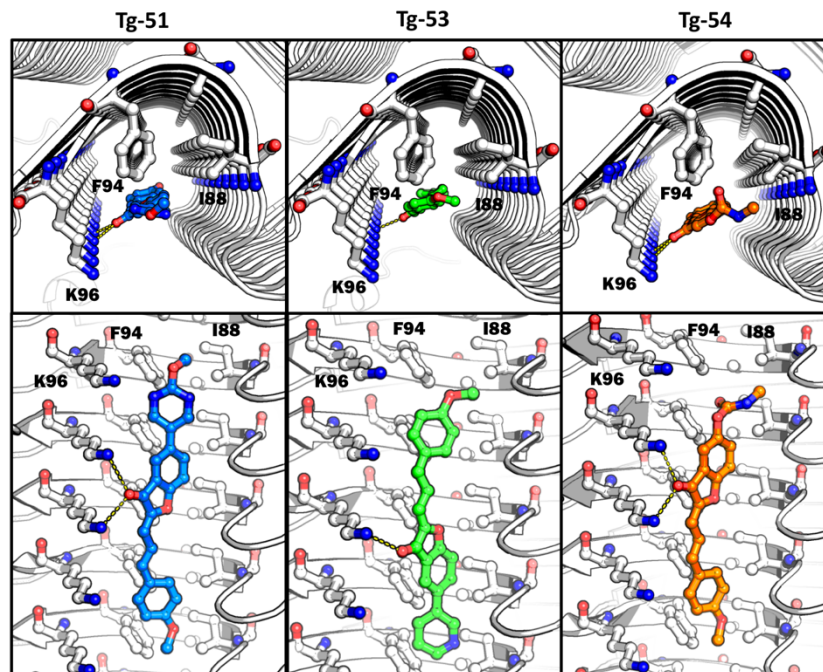


Figure S3. Docking of **Tg-51**, **Tg-53** and **Tg-54** binding to site 9 in α -Syn, viewed from the fibril axis (top) and from the side (bottom).

Table S1. Probability and predicted binding energy of two putative binding sites.

	Binding Site	2	9
Tg-51	Probability (%)	40.40%	13.40%
	Average BE (kcal/mol)	-7.43±0.27	-7.80±0.28
	Best BE (kcal/mol)	-7.87	-8.32
Tg-52	Probability (%)	41.30%	19.30%
	Average BE (kcal/mol)	-7.72±0.27	-8.22±0.28
	Best BE (kcal/mol)	-8.30	-8.71
Tg-53	Probability (%)	40.20%	18.30%
	Average BE (kcal/mol)	-7.36±0.14	-8.29±0.27
	Best BE (kcal/mol)	-7.54	-8.76
Tg-54	Probability (%)	36.80%	15.30%
	Average BE (kcal/mol)	-6.70±0.41	-6.89±0.41
	Best BE (kcal/mol)	-7.54	-7.81

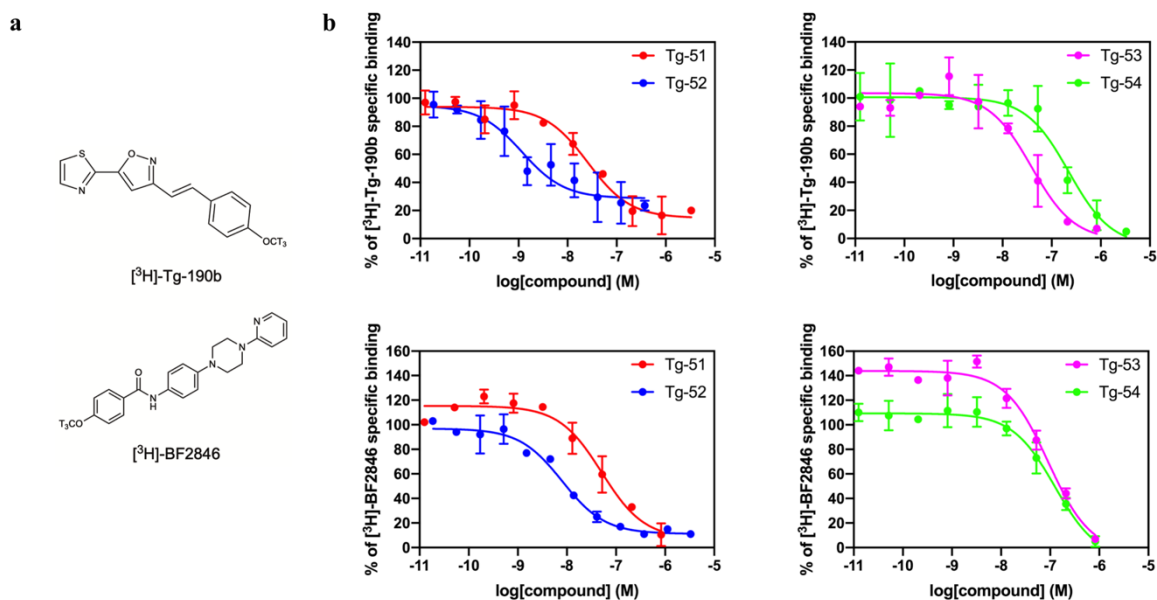


Figure S4. (a) Molecular structures of radioligands, $[^3\text{H}]\text{-Tg-190b}$ and $[^3\text{H}]\text{-BF2846}$, used in the competition binding assay. (b) Competition binding curves for compounds **Tg-51**, **Tg-52**, **Tg-53** and **Tg-54**. $\alpha\text{-Syn}$ fibrils were incubated with fixed concentrations of $[^3\text{H}]\text{-Tg-190b}$ or $[^3\text{H}]\text{-BF2846}$ and increasing concentrations of competitors. Data points represent mean \pm s.d. ($n=3$).

Table S2. Examples for previously reported fluorescent $\alpha\text{-Syn}$ ligands and their binding affinity.

$\alpha\text{-Syn}$ Ligand	Measured Affinity
Thioflavin T ⁶⁻⁷	$K_d = 0.95 \pm 0.27 \mu\text{M}^*$ for $\alpha\text{-Syn}$ fibrils * Many publications report the K_d of ThT binding to $\alpha\text{-syn}$ fibrils and reported values range from $0.5 \mu\text{M}$ to $15 \mu\text{M}$. Differences in K_d values may be explained by differences in $\alpha\text{-Syn}$ fibril preparation and incubation conditions. ⁷ $K_i = 1.04 (0.755\text{-}1.44) \mu\text{M}^*$ *95% confidence intervals for K_i values are shown in parentheses.
SL-631 ⁸	Dye to $\alpha\text{-syn}$ oligomer binding constant: $3.8 \pm 0.5 \times 10^5 \text{ M}^{-1}$ * *saturation was not reached at the experiment
$[^{18}\text{F}]\text{46a}$ ⁹	$K_d = 8.9 \times 10^{-3} \mu\text{M}$ for $\alpha\text{-Syn}$ fibrils
bis-ANS ¹⁰	$K_d = 8.6 \pm 0.5 \mu\text{M}$ for $\alpha\text{-Syn}$ fibrils
T-284	$K_d = 0.56 \mu\text{M}$ for $\alpha\text{-Syn}$ fibrils
SH-516 ¹¹	$K_d = 0.65 \mu\text{M}$ for $\alpha\text{-Syn}$ fibrils
TPE-TPP ¹²	$K_d = 4.36 \mu\text{M}$ for $\alpha\text{-Syn}$ fibrils

Table S3. Absorbance and Fluorescence Maxima, Extinction Coefficients, Quantum Yields, Brightness and Lifetimes for Tg-51-54 Compounds.

Compound	Absorbance λ_{\max} (nm)		Bound Fluorescence λ_{\max} (nm)		Ext. Coeff. (ϵ , M ⁻¹ cm ⁻¹)		Quantum Yield (Φ)*	Brightness ($\epsilon \cdot \phi$, M ⁻¹ cm ⁻¹)	Lifetime (ns)
	Free	Bound	Ex.	Em.	Free	Bound*	Bound	Bound	Bound
Tg-51	362	448	449	523	7090	41860	0.007	123	1.11
Tg-52	435	448	451	522	7307	37360	0.003	57	1.16
Tg-53	435	448	452	534	15320 [†]	60890	0.005	127	1.00
Tg-54	437	446	451	529	29510	36610	0.004	71	1.08

* The bound extinction coefficients along with the quantum yield values were determined based on the absolute absorbance values and estimations of bound concentration. They were also determined by comparison to ThT values reported in *Sulatskaya et al.*¹³ The values determined in this fashion differed by roughly 2-fold. We note that since the compounds are essentially non-fluorescent in the unbound state in aqueous solvent, we were not able to determine a Free quantum yield.

[†] The linear regression of single-wavelength absorbances of serially diluted **Tg-53** was fit with a y-intercept value of 0.11 and the reported extinction coefficient represents the slope of the linear absorbance range for this compound.

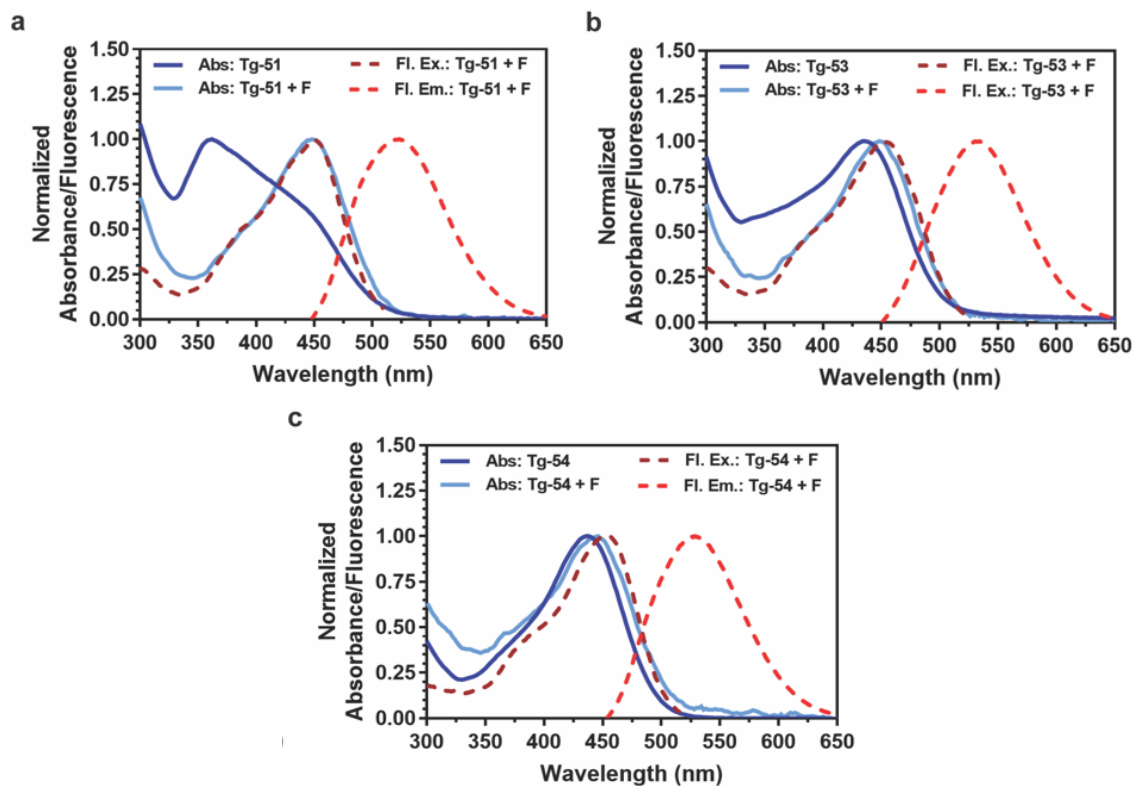


Figure S5. Absorbance and emission spectra of Tg compounds free in solution and bound to fibrils. Absorbance spectra of each compound free in solution (blue solid line) and bound to α -Syn fibrils (light-blue solid line) along with the bound fluorescence excitation spectrum (dark red dashed line) and emission spectrum (red dashed line) were acquired with 1 μ M of either **Tg-51** (a), **Tg-53** (b) or **Tg-54** (c) and 98 μ M α -Syn fibrils.

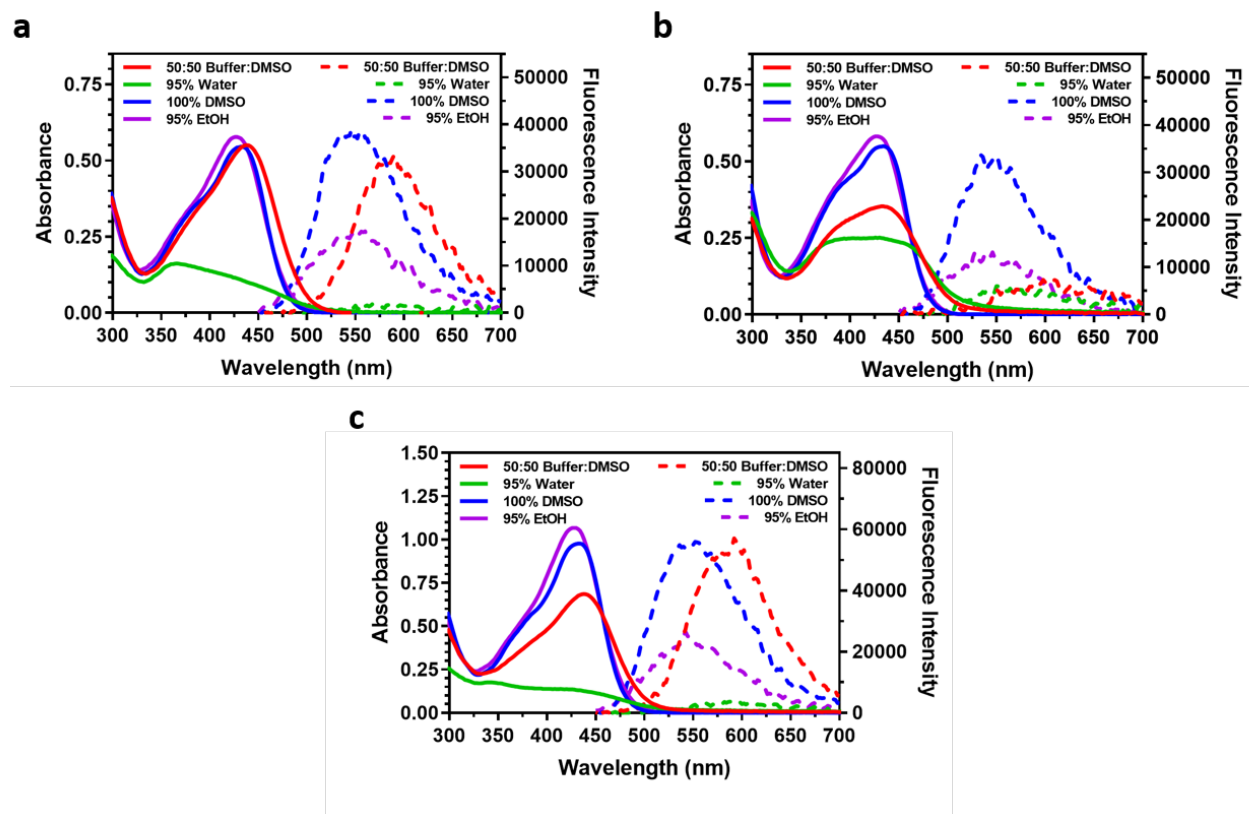


Figure S6. Absorbance and fluorescence spectra of Tg compounds in solvents with varying polarity. Absorbance (solid lines) and fluorescence (dashed lines) spectra of **Tg-51** (a), **Tg-53** (b) and **Tg-54** (c) in 50:50 buffer:DMSO (red), 95% water (green), 100 % DMSO (blue) and 95% ethanol (purple). Absorbance and fluorescence spectra were acquired at 20 μ M and 5 μ M concentrations of the compounds, respectively.

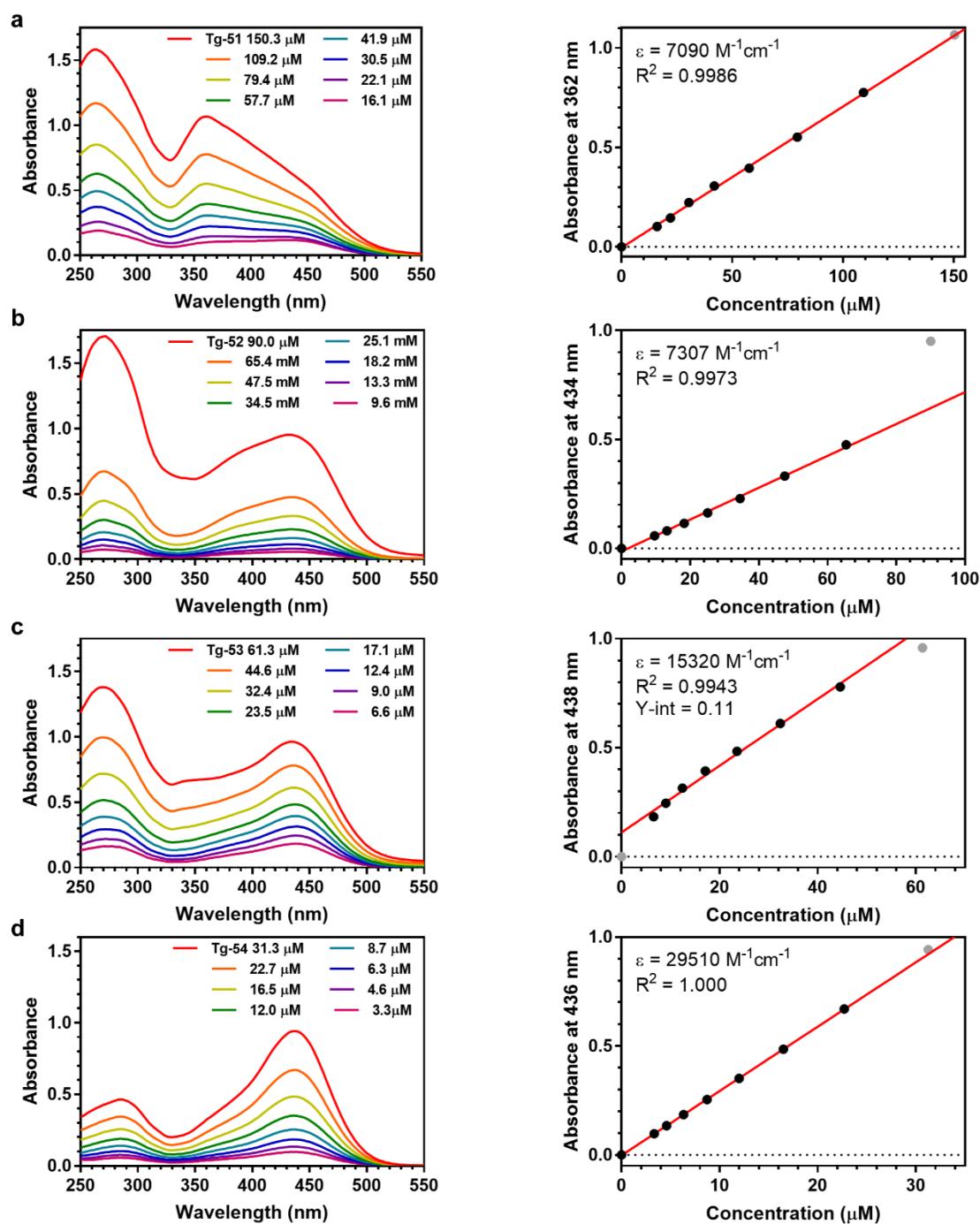


Figure S7. Determination of extinction coefficient of Tg compounds. Absorbance spectra of **Tg-51** (a), **Tg-52** (b), **Tg-53** (c) and **Tg-54** (d) were acquired at 1 μM in 50:50 buffer:DMSO. The absorbance spectra from serial dilutions of each compound (left) were used to compute extinction coefficients for each compound at the absorbance maxima in the 350-350 nm range via linear regression (right). Points shown in black were used in the linear regression to obtain the extinction coefficient (slope) whereas points in grey display deviations from linearity suggesting possible aggregation.

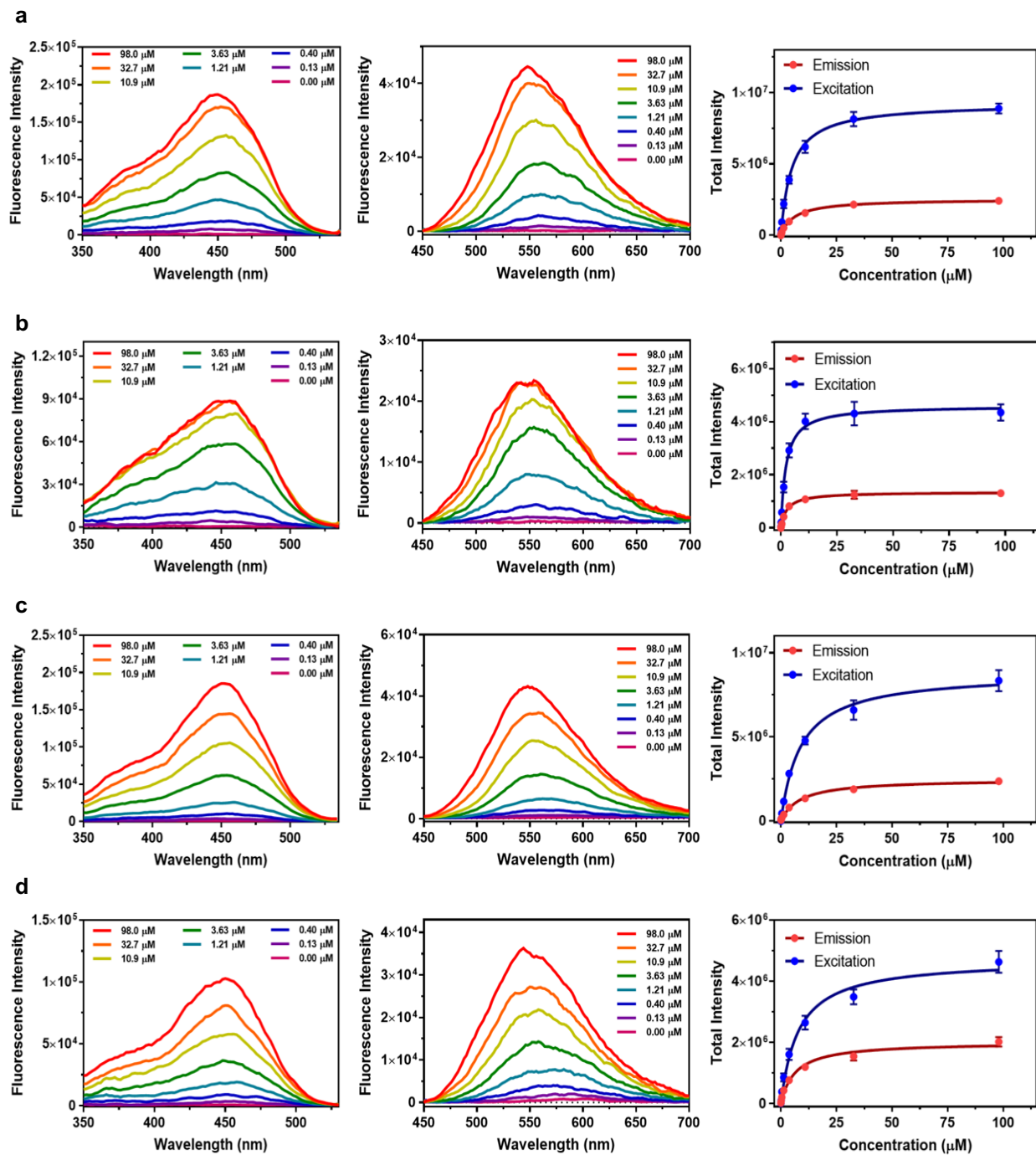


Figure S8. Determination of fluorescence turn-on of Tg compounds from fibril binding. Fluorescence excitation (left) and emission spectra (middle) were acquired for 1 μ M **Tg-51** (a), **Tg-52** (b), **Tg-53** (c) and **Tg-54** (d) in the presence of serial dilutions of α -Syn fibrils. The integrated total fluorescence intensity for each compound as a function of fibril concentration (right) was fit to Equation 1 for both the excitation (blue) and emission (red) measurements with fitting parameters displayed in Table 2.

Table S4. Fitting parameters from fibril binding induced turn-on of the compounds.

Compound	Excitation					Emission				
	B _{max}		Relative K _d		R ²	B _{max}		Relative K _d		R ²
Average	Std. Error	Average	Std. Error	Average		Std. Error	Average	Std. Error		
Tg-51	9248648	181677	4.78	0.372	0.997	2528386	47936	6.03	0.435	0.998
Tg-52	4600756	93499	2.23	0.204	0.996	1342302	18993	2.69	0.166	0.998
Tg-53	8810469	244172	8.83	0.861	0.996	2476602	79118	8.53	0.967	0.995
Tg-54	4715121	234484	7.77	1.397	0.987	2009778	107596	6.31	1.273	0.983

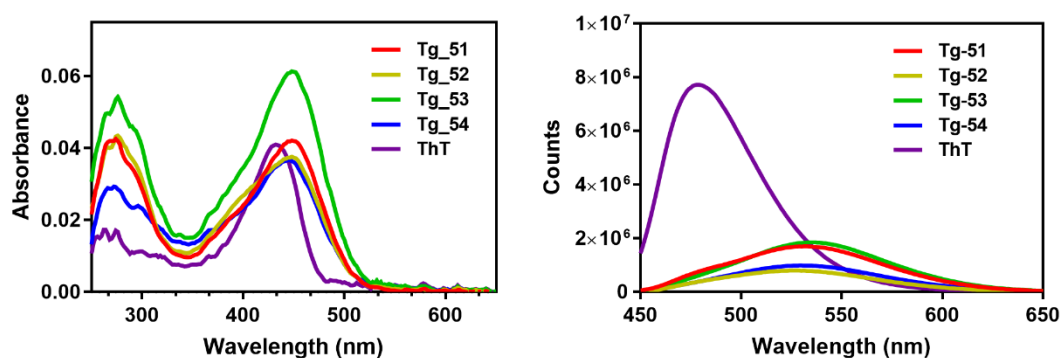


Figure S9. Determination of Quantum Yield of Tg Compounds using Thioflavin T (ThT) as a Standard. Absorbance and fluorescence emission spectra were acquired for 1 μ M **Tg-51** (red), **Tg-52** (yellow), **Tg-53** (green), **Tg-54** (blue) and ThT (purple) in the presence of 98 μ M α -Syn fibrils. Absorbance and emission spectra of 98 μ M α -Syn fibrils were subtracted from all measurements.

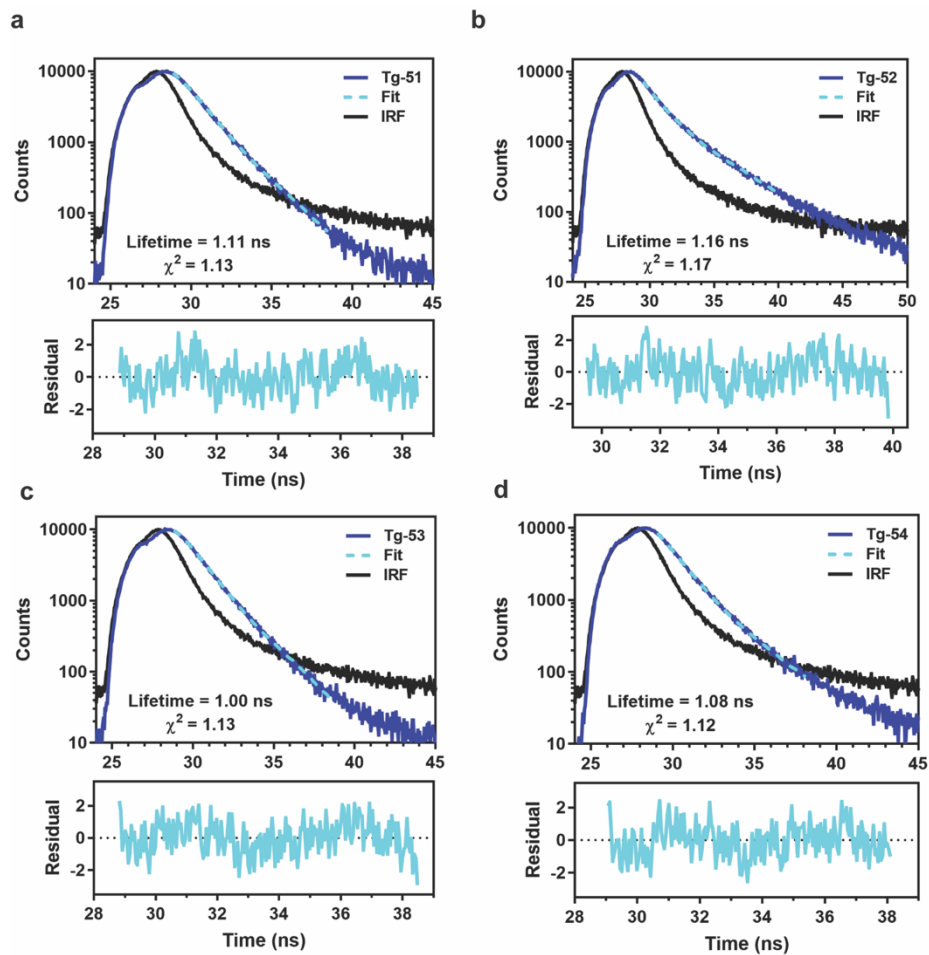


Figure S10. Determination of fluorescence lifetime of compounds bound to fibrils. Time-correlated single photon counting (TCSPC) experiments and the resultant histograms were fit to single-exponential decays to capture the fluorescence lifetime of **Tg-51** (a), **Tg-52** (b), **Tg-53** (c) and **Tg-54** (d) bound to α -Syn fibrils.

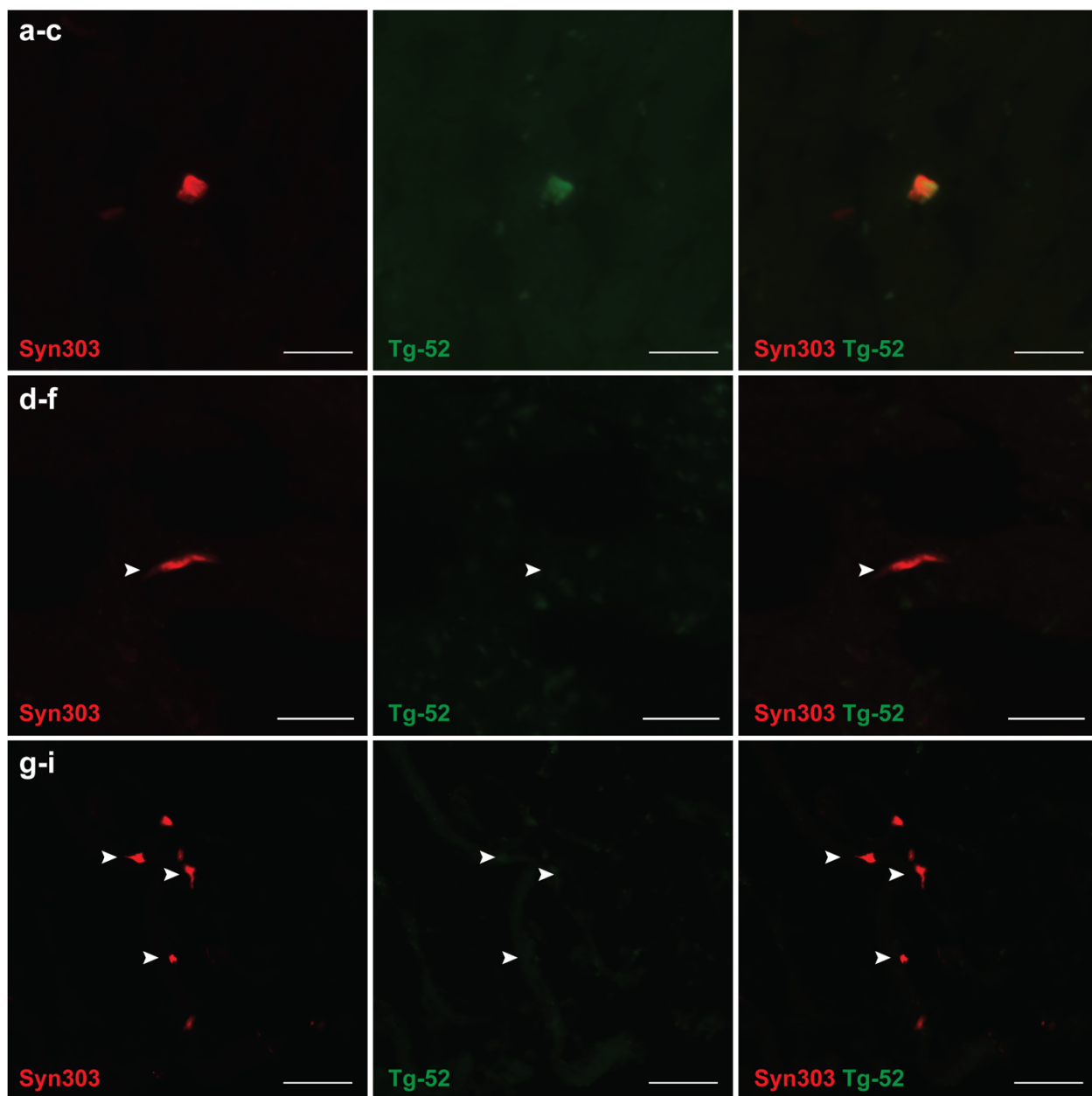


Figure S11. Fluorescence microscopy studies of compound **Tg-52** in post-mortem samples of PD and MSA brain. Images show LBs (a-c), LNs (d-f) and GCIs (g-i) immunostained with Syn303 antibody and **Tg-52**. The fluorescent compound shows high labeling of LBs. [Scale bars, 50 μ m (a-c), 20 μ m (d-f) and 50 μ m (g-i)]

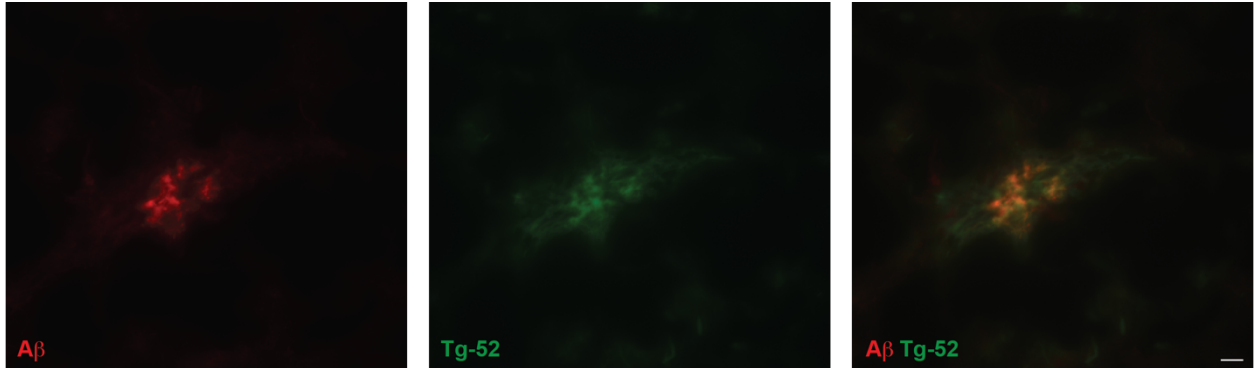


Figure S12. Fluorescent microscopy studies of **Tg-52** in post-mortem samples of AD brain. Brain sections were immunostained with anti-A β antibody, followed by incubation with 10 μ M **Tg-52** for 2 hours (scale: 20 μ m).

References

1. C. M. Haney, R. F. Wissner, J. B. Warner, Y. J. Wang, J. J. Ferrie, D. J. Covell, R. J. Karpowicz, V. M.-Y. Lee and E. J. Petersson, *Org. Biomol. Chem.*, 2016, **14**, 1584-1592.
2. A. I. Sulatskaya, N. P. Rodina, M. I. Sulatsky, O. I. Povarova, I. A. Antifeeva, I. M. Kuznetsova and K. K. Turoverov, *Int. J. Mol. Sci.*, 2018, **19**, 2486.
3. (a) J. Brettschneider, K. Del Tredici, V. M.-Y. Lee and J. Q. Trojanowski, *Nat. Rev. Neurosci.*, 2015, **16**, 109; (b) J. B. Toledo, V. M. Van Deerlin, E. B. Lee, E. Suh, Y. Baek, J. L. Robinson, S. X. Xie, J. McBride, E. M. Wood and T. Schuck, *Alzheimer's & dementia*, 2014, **10**, 477-484. e471; (c) J. L. Robinson, E. B. Lee, S. X. Xie, L. Rennert, E. Suh, C. Bredenberg, C. Caswell, V. M. Van Deerlin, N. Yan and A. Yousef, *Brain*, 2018, **141**, 2181-2193.
4. C.-J. Hsieh, J. J. Ferrie, K. Xu, I. Lee, T. J. Graham, Z. Tu, J. Yu, D. Dhavale, P. Kotzbauer and E. J. Petersson, *ACS Chem. Neurosci.*, 2018, **9**, 2521-2527.
5. G. M. Morris, R. Huey, W. Lindstrom, M. F. Sanner, R. K. Belew, D. S. Goodsell and A. J. Olson, *J. Comput. Chem.*, 2009, **30**, 2785-2791.
6. L. Yu, J. Cui, P. K. Padakanti, L. Engel, D. P. Bagchi, P. T. Kotzbauer and Z. Tu, *Bioorg. Med. Chem.*, 2012, **20**, 4625-4634.
7. D. P. Bagchi, L. Yu, J. S. Perlmutter, J. Xu, R. H. Mach, Z. Tu and P. T. Kotzbauer, *PLoS one*, 2013, **8**, e55031.
8. V. Kovalska, M. Y. Losytskyy, O. Tolmachev, Y. L. Slominskii, G. M. Segers-Nolten, V. Subramaniam and S. Yarmoluk, *J. Fluoresc.*, 2012, **22**, 1441-1448.
9. W. Chu, D. Zhou, V. Gaba, J. Liu, S. Li, X. Peng, J. Xu, D. Dhavale, D. P. Bagchi and A. d'Avignon, *J. Med. Chem.*, 2015, **58**, 6002-6017.
10. M. S. Celej, E. A. Jares-Erijman and T. M. Jovin, *Biophysical journal*, 2008, **94**, 4867-4879.
11. K. D. Volkova, V. Kovalska, A. Balanda, M. Y. Losytskyy, A. Golub, R. Vermeij, V. Subramaniam, O. Tolmachev and S. Yarmoluk, *Bioorg. Med. Chem.*, 2008, **16**, 1452-1459.
12. C. W. T. Leung, F. Guo, Y. Hong, E. Zhao, R. T. K. Kwok, N. L. C. Leung, S. Chen, N. N. Vaikath, O. M. El-Agnaf and Y. Tang, *Chem. Commun.*, 2015, **51**, 1866-1869.
13. A. Sulatskaya, N. Rodina, M. Sulatsky, O. Povarova, I. Antifeeva, I. Kuznetsova and K. Turoverov, *Int. J. Mol. Sci.*, 2018, **19**, 2486.